

Multi-Server Over-the-Air Federated Learning

Seyed Mohammad Azimi-Abarghouyi and Viktoria Fodor

Abstract

In this work, we propose a communication-efficient two-layer federated learning algorithm for distributed setups including a core server and multiple edge servers with clusters of devices. Assuming different learning tasks, clusters with a same task collaborate. To implement the algorithm over wireless links, we propose a scalable clustered over-the-air aggregation scheme for the uplink with a bandwidth-limited broadcast scheme for the downlink that requires only two single resource blocks for each algorithm iteration, independent of the number of edge servers and devices. This setup is faced with interference of devices in the uplink and interference of edge servers in the downlink that are to be modeled rigorously. We first develop a spatial model for the setup by modeling devices as a Poisson cluster process over the edge servers and quantify uplink and downlink error terms due to the interference. Accordingly, we present a comprehensive mathematical approach to derive the convergence bound for the proposed algorithm including any number of collaborating clusters in the setup and provide important special cases and design remarks. Finally, we show that despite the interference in the proposed uplink and downlink schemes, the proposed algorithm achieves high learning accuracy for a variety of parameters.

Index Terms

Federated learning, machine learning, multi-server systems, clustered networks, over-the-air computation.

I. INTRODUCTION

With the growing pervasiveness and computational power of wireless edge devices, i.e., phones, smart watches, sensors, and autonomous vehicles, there is an increasing demand for enabling machine learning to train a global model from the diverse distributed data over the edge devices [1], [2]. However, loading such enormous amounts of data from the devices to a central server is not often feasible due to strict constraints on latency, power, and bandwidth, or concerns on data privacy. A promising and practically feasible distributed approach is federated

The authors are with the School of Electrical Engineering and Computer Science, KTH Royal Institute of Technology, Stockholm, Sweden (Emails: {seyaa,vjfodor}@kth.se).

learning (FL), which is able to implement machine learning directly at the wireless edge while under no circumstances the data leaves the devices [3], [4]. In this approach, the model training is performed locally at each single device with the help of a parameter server, such that synchronous model update at all devices and model aggregation at the server are repeated until convergence. Most studies on FL consider a single server [5]–[7]. However, to support more devices that can collaborate in the learning process, some recent studies have proposed hierarchical architectures for FL that incorporate a core server and multiple edge servers [8]–[12]. The hierarchical FL has two layers of aggregation of model parameters: the synchronous aggregation at the edge servers and then a global aggregation at the core server to coordinate the edge servers. In large scale systems, the hierarchical FL has less communication overhead and latency in comparison with the single-server architecture.

In reality, the FL requires transmissions over unreliable wireless networks under given limited resources and power constraints. In these networks, many devices and the edge server communicate with each other through a shared wireless propagation medium. Hence, communication efficiency is one of the most crucial challenges in the FL. As the conventional approach, orthogonal digital multiple access techniques have been utilized in FL via individual transmissions of different devices to the server. This causes significant communication latency and resource requirements [13], [14]. A desirable and efficient strategy is referred to as over-the-air FL which uses the over-the-air computation scheme [15], [16] to harness interference from simultaneous multi-access transmissions of edge devices for the purpose of aggregation [17]–[21]. By integrating communication and computation, the over-the-air FL has the ability to operate under remarkably less resources and communication and computation latencies than the FL with orthogonal transmissions. This leads to better learning accuracy and efficiency under wireless channel hostilities and the scarcity of resources [22]. There is a hierarchical over-the-air FL scheme in [12] that leverages multiple antennas and perfect channel knowledge at the servers. The aforementioned works on the over-the-air FL consider and attempt to compensate for errors due to the unreliable uplink transmissions, but assume ideal error-free server-to-devices downlink. There are two studies [23], [24] that consider practical bandwidth limited downlink for single- and multi-cell wireless networks, respectively. Moreover, works on the hierarchical FL [8]–[11] are based on orthogonal transmissions.

This paper develops a comprehensive design and analysis for multi-server FL systems including a core server and clusters of devices, each cluster with an edge server. Our key contributions

are highlighted next.

Learning Framework: We propose a new iterative learning method with a two-layer aggregation named MultiAirFed. In MultiAirFed, first a number of intra-cluster gradient aggregations are performed by the edge server within each cluster. Then, the clusters that have the same task perform an inter-cluster aggregation of the model parameters, with the help of the core server.

Transmission Scheme: Under limited transmit powers at the devices and the servers, we propose a scalable clustered over-the-air aggregation scheme for the uplink and a bandwidth-limited broadcast scheme for the downlink. The proposed schemes are analog and perform under interference from simultaneous transmissions. Using the schemes, we implement MultiAirFed over a large-scale wireless network where independent of the number of clusters and devices, each iteration all over the network is performed only in two single resource blocks, one for the uplink and one for the downlink. Different from the literature where mostly ideal error-free orthogonal downlink links are assumed [5]–[12], [18], [19], we consider imperfect bandwidth-limited downlink broadcast links as common in wireless networks [26], [31]. It is notable that orthogonal downlink transmission is not often a feasible approach in large-scale networks as it requires a huge bandwidth in support of all the nodes.

Tractable Modeling and Convergence Analysis: For rigorous modeling and analysis, a thorough enough spatial model is required to take into account the principal features of the setup while being tractable to enable mathematical analysis of the interference and its effect on the convergence performance. Inspired by this fact, we use Poisson cluster processes (PCPs) [25]–[28] to model the correlation that exists between the locations of the devices and servers in clusters. PCPs have numerous applications in clustered networks [26], [29]. According to the model, we comprehensively characterize the learning convergence in terms of the optimality gap for the setup and present design remarks and special cases. As a key step for the convergence analysis, we quantify uplink and downlink error terms, due to interference, in recovering the intra- and inter-cluster aggregations. We also investigate the effects of the uplink and downlink errors on the optimality gap. To highlight the novelty of this analysis, please note that the proposed MultiAirFed algorithm is new including two different gradient and model parameters uploads and updates. Also, the convergence analysis in the literature for the hierarchical FL has been limited to the ideal communication setups with orthogonal transmissions and fixed number of active devices.

System Design Insights: Our analysis reveals that a higher density of cluster centers has a

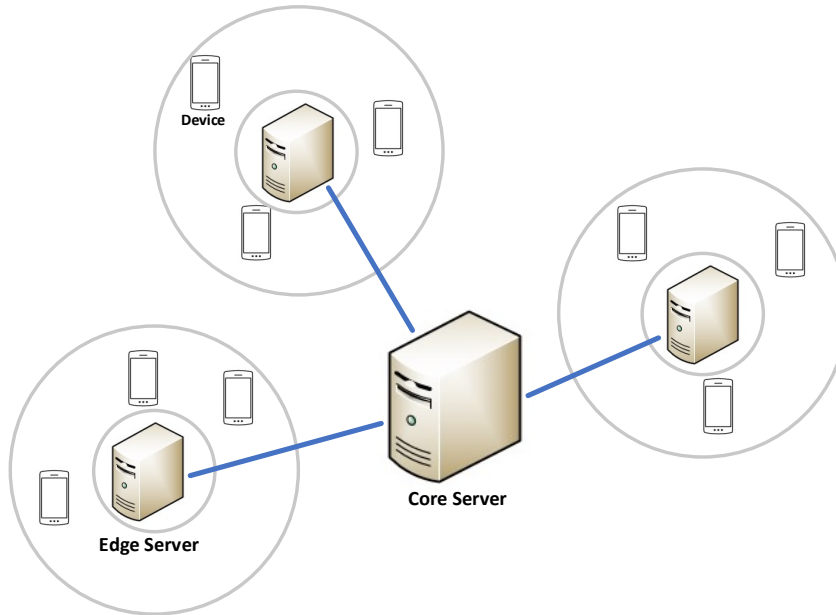


Fig. 1: Multi-server FL system, where three clusters are illustrated.

degrading effect on the learning performance. Also, increasing the number of devices in each cluster or the number of collaborating clusters in the learning process increases the learning accuracy, however, the improvement is limited by increasing the interference. Furthermore, although more intra-cluster iterations improve the accuracy, it does not necessarily decrease the learning latency. Moreover, the proposed algorithm can provide significantly better learning accuracy compared to other hierarchical FL algorithms in the proposed wireless setup.

II. SYSTEM MODEL

In this section, we provide a mathematical model of the system, including the distribution of devices and servers, and the channel model.

A. Network Topology

We consider a multi-server FL system as shown in Fig. 1, where the locations of edge devices are modeled as a PCP on an infinite 2D space [25]. In the center of each cluster, there is an edge server that helps the learning process of the edge devices of the same cluster.

A PCP Φ is formally defined as a union of offspring points in \mathbb{R}^2 that are located around parent points, i.e., cluster centers. The parent point process is a homogeneous Poisson point process (PPP) Φ_p with density λ_p . Also, the offspring point processes are conditionally independent. The

set of offspring points of $\mathbf{x} \in \Phi_p$ is denoted by cluster $\mathcal{N}^{\mathbf{x}}$, such that $\Phi = \cup_{\mathbf{x} \in \Phi_p} \mathcal{N}^{\mathbf{x}}$. The PDF of each element of $\mathcal{N}^{\mathbf{x}}$ being at a location $\mathbf{y} + \mathbf{x} \in \mathbb{R}^2$ inside the cluster is shown by $f_{\|\mathbf{y}\|}(y)$.

In wireless networks, clusters are mostly modeled as disk-shaped regions where nodes are distributed uniformly. When these clusters are employed in a PCP such that offspring points are distributed randomly and uniformly in disks centered at parent points, the resulting point process is referred to as Matérn cluster process (MCP) [25]. Also, since the edge servers are usually located inside base station buildings or integrated with antenna towers, there are protective zones over them where devices and other edge servers cannot be located. Therefore, we further consider a modified type of MCP, named MCP with holes at the cluster centers (MCP-H) [27], where the points are distributed around cluster centers with uniform distribution inside rings with inner radius r_0 and outer radius R as

$$f_{\|\mathbf{y}\|}(y) = \frac{2y}{R^2 - r_0^2}, \quad r_0 \leq y \leq R. \quad (1)$$

The number of devices in each cluster is assumed to be M , i.e., $|\mathcal{N}^{\mathbf{x}}| = M$. Also, among all the devices of a cluster \mathbf{x} , the set of active devices in a time slot is denoted by $\mathcal{A}^{\mathbf{x}} \subset \mathcal{N}^{\mathbf{x}}$. The term "active device" denotes a device that participates in the aggregation phase of the FL by its uplink transmission. We assume that there is at least one active device in each cluster.

We consider that clusters may have different or similar learning tasks. For example, a university campus is mostly interested in science learning tasks in contrast with a farm where the type of sensors and data are completely different. We also consider that there is a core server connected to the edge servers by backhaul links to help the learning process of all the clusters when needed. Clusters with the same task collaborate through the core server.

B. Channel Model

All the nodes are single-antenna units. The communication between the edge servers and the core server is considered error free. However, for the wireless links between devices and edge servers, we assume single-slope power-law path loss and small-scale i.i.d. Rayleigh fading. The pathloss exponent is denoted by parameter α . The uplink fading between a device $\mathbf{y} \in \mathcal{N}^{\mathbf{x}}$ and a server at \mathbf{z} is modeled by $f_{\mathbf{yz}}^{\mathbf{x}} \in \mathbb{C}$, such that the channel gain $|f_{\mathbf{yz}}^{\mathbf{x}}|^2 \sim \exp(1)$. Also, the downlink fading between a server \mathbf{x} and a representative device is $f^{\mathbf{x}}$ with the gain $|f^{\mathbf{x}}|^2 \sim \exp(1)$. However, the downlink channel gains from an edge server to the devices of its cluster are assumed to be higher than a threshold th_0 . Also, all channel gains are assumed invariant during

one time slot required for a transmission, while they change independently from one time slot to another.

III. PROPOSED LEARNING FRAMEWORK

Assume that there are C collaborating clusters including a representative cluster with its center at the origin \mathbf{o} that have a same learning task. The centers of these clusters are denoted by a set \mathcal{C} . Also, a device at a location \mathbf{y} in a cluster \mathbf{x} has its local private dataset $\mathcal{D}_y^{\mathbf{x}}$. The l -th sample in $\mathcal{D}_y^{\mathbf{x}}$ is denoted by ξ_l . The learning model is parametrized by the parameter vector $\mathbf{w} \in \mathbb{R}^d$ with $\mathbf{w} = [w_1, \dots, w_d]^T$, where d denotes the learning model size. Then, the local loss function of the model parameter vector \mathbf{w} over $\mathcal{D}_y^{\mathbf{x}}$ is

$$F_y^{\mathbf{x}}(\mathbf{w}) = \frac{1}{D} \sum_{\xi_l \in \mathcal{D}_y^{\mathbf{x}}} f(\mathbf{w}, \xi_l), \quad (2)$$

where D is the dataset size for each device, i.e., $D = |\mathcal{D}_y^{\mathbf{x}}|, \forall \mathbf{y}, \mathbf{x}$ ¹ and $f(\mathbf{w}, \xi_l)$ is the sample-wise loss function that quantifies the prediction error of the model vector \mathbf{w} on the sample ξ_l . Then, the global loss function on the distributed datasets $\cup_{\mathbf{x} \in \mathcal{C}} \cup_{\mathbf{y} \in \mathcal{N}^{\mathbf{x}}} \mathcal{D}_y^{\mathbf{x}}$ over the clusters in \mathcal{C} is computed as

$$F(\mathbf{w}) = \sum_{\mathbf{x} \in \mathcal{C}} \sum_{\mathbf{y} \in \mathcal{N}^{\mathbf{x}}} F_y^{\mathbf{x}}(\mathbf{w}). \quad (3)$$

Thus, the learning process has the objective to find a desired model parameter vector \mathbf{w} that minimizes $F(\mathbf{w})$ as

$$\mathbf{w}^* = \min_{\mathbf{w}} F(\mathbf{w}). \quad (4)$$

In general, FL algorithms solve (4) in two steps: local update and aggregation. These steps are distributedly repeated over a number of iterations based on gradient descent techniques [3], [4].

In this paper, we propose a new two-layer algorithm named `MultiAirFed` for the multi-server systems as follows. Consider T global inter-cluster iterations. In a particular iteration t , consider τ intra-cluster iterations. In a particular intra-cluster iteration i , each device \mathbf{y} in a cluster \mathbf{x} computes the local gradient of the loss function in (2) from its local dataset, indexed by $\{i, t\}$, as

$$\mathbf{g}_{y,i,t}^{\mathbf{x}} = \frac{1}{D} \sum_{\xi_l \in \mathcal{D}_y^{\mathbf{x}}} \nabla f(\mathbf{w}, \xi_l). \quad (5)$$

¹This is for simplicity. Extension to different dataset sizes is straightforward.

Then, devices upload (transmit) their local gradients to their servers for intra-cluster aggregation phase. As the aggregation, the intra-cluster gradient of cluster \mathbf{x} at its server is obtained with the average of local gradients from its active devices as

$$\mathbf{g}_{i,t}^{\mathbf{x}} = \frac{1}{|\mathcal{A}_{i,t}^{\mathbf{x}}|} \sum_{\mathbf{y} \in \mathcal{A}_{i,t}^{\mathbf{x}}} \mathbf{g}_{\mathbf{y},i,t}^{\mathbf{x}}, \quad (6)$$

where $|\mathcal{A}_{i,t}^{\mathbf{x}}|$ is the number of active devices in the cluster \mathbf{x} for the iteration index $\{i, t\}$. Then, the servers broadcast back the intra-cluster gradients $\mathbf{g}_{i,t}^{\mathbf{x}}, \forall \mathbf{x}$ to their devices. Based on $\mathbf{g}_{i,t}^{\mathbf{x}}$, each device \mathbf{y} in any cluster \mathbf{x} synchronously updates its local learning model following the gradient descent as

$$\mathbf{w}_{\mathbf{y},i+1,t}^{\mathbf{x}} = \mathbf{w}_{\mathbf{y},i,t}^{\mathbf{x}} - \mu_t \mathbf{g}_{i,t}^{\mathbf{x}}, \quad (7)$$

where μ_t is the learning rate at the global iteration t . After completing τ intra-cluster iterations, devices upload their model parameters, i.e., $\mathbf{w}_{\mathbf{y},\tau,t}^{\mathbf{x}}, \forall \mathbf{y}, \mathbf{x}$, to their servers. Accordingly, each server \mathbf{x} computes an intra-cluster model parameter vector with the following average

$$\mathbf{w}_{t+1}^{\mathbf{x}} = \frac{1}{|\mathcal{A}_{\tau,t}^{\mathbf{x}}|} \sum_{\mathbf{y} \in \mathcal{A}_{\tau,t}^{\mathbf{x}}} \mathbf{w}_{\mathbf{y},\tau,t}^{\mathbf{x}}. \quad (8)$$

Then, collaborating servers upload their intra-cluster model parameter vectors to the core server for a global inter-cluster model parameter aggregation as

$$\mathbf{w}_{t+1}^{\mathbf{G}} = \frac{1}{|\mathcal{A}_{\tau,t}|} \sum_{\mathbf{x} \in \mathcal{C}} |\mathcal{A}_{\tau,t}^{\mathbf{x}}| \mathbf{w}_{t+1}^{\mathbf{x}}, \quad (9)$$

which is the average of all model parameter vectors from the active devices in the clusters of \mathcal{C} . Also, $|\mathcal{A}_{\tau,t}| = \sum_{\mathbf{x} \in \mathcal{C}} |\mathcal{A}_{\tau,t}^{\mathbf{x}}|$ denotes the number of the active devices for the iteration index $\{\tau, t\}$. Then, the servers broadcast $\mathbf{w}_{t+1}^{\mathbf{G}}$ to the devices to update their initial state of model parameter vector for the next global iteration $t + 1$ as $\mathbf{w}_{\mathbf{y},0,t+1}^{\mathbf{x}} = \mathbf{w}_{t+1}^{\mathbf{G}}, \forall \mathbf{y}, \mathbf{x}$. This global update is also to synchronize all the devices from different collaborating clusters in the learning process. This prevents a high deviation of local training in different clusters. The algorithm is presented in Algorithm 1.

The MultiAirFed utilizes one local update at the devices per iteration like FedSGD [3]. Such solution showed to be robust to heterogeneity and non-i.i.d. data [30]. Extension to multiple local updates at the devices like FedAvg [3] is possible. To keep the convergence analysis tractable, we leave this extension for future work. Also, compared to other hierarchical methods in [8]–[12] which are based on model parameter transmissions, gradient transmission in MultiAirFed

over wireless links is expected to be more robust to channel noise. This is because a noisy model parameter estimation contributes imperfections on both the initial state and a non-linear gradient evaluation for the local update (7) in the devices. This will be further justified through experimental results in Fig. 7.

Before conclusion of this discussion, note that the proposed learning framework is not limited to the choice of the spatial model in Subsection II.A, which is a popular model, and can be easily applied to general setups of multi-server FL systems.

Algorithm 1 MultiAirFed algorithm

Initialize the global model \mathbf{w}_0^G

for inter-cluster iteration $t = 1, \dots, T$ **do**

Each device updates its model by \mathbf{w}_t^G

for intra-cluster iteration $i = 1, \dots, \tau$ **do**

Each device obtains local gradient from (5)

Each server obtains intra-cluster gradient from (6)

Each device updates its local model as in (7)

Each server obtains intra-cluster model from (8)

Core server obtains global model \mathbf{w}_{t+1}^G from (9)

IV. CLUSTERED TRANSMISSION SCHEME

To implement MultiAirFed, we propose a scalable scheme including two types of analog transmissions for uplink and downlink, where each is done synchronically over all clusters of the network in a single resource block. It is inspired from [23] which shows that analog downlink approach significantly outperforms the digital one. From here, we ignore the iteration indexes for simplicity of presentation, except where needed.

A. Uplink

For the uplink, we propose a clustered over-the-air aggregation scheme. The term "over-the-air" is from the facts that devices transmit simultaneously and the objective is to construct the aggregation vectors (6) and (9) at the edge servers based on the additive nature of wireless multiple-access channels. The term "clustered" comes from the fact that the transmission in each cluster is independent from other clusters.

To be able to concentrate on the effect of interference, we assume i.i.d. data over devices in each cluster \mathbf{x} , as accepted in the literature, e.g., [18], [19]. Therefore, depending on an intra- or inter-cluster iteration, the distribution of the gradient parameters or model parameters at each device of the cluster is assumed to have known variance and mean $(\sigma_{\mathbf{g},\mathbf{x}}^2, \mu_{\mathbf{g},\mathbf{x}})$ or $(\sigma_{\mathbf{w},\mathbf{x}}^2, \mu_{\mathbf{w},\mathbf{x}})$, respectively. Then, for an intra-cluster iteration, the local gradient vector at a device $\mathbf{y} \in \mathcal{N}^{\mathbf{x}}$, i.e., $\mathbf{g}_{\mathbf{y}}^{\mathbf{x}}$, is normalized before transmission to have zero mean and unit variance, i.e., $\bar{\mathbf{g}}_{\mathbf{y}}^{\mathbf{x}} = \frac{\mathbf{g}_{\mathbf{y}}^{\mathbf{x}} - \mu_{\mathbf{g},\mathbf{x}}}{\sigma_{\mathbf{g},\mathbf{x}}}$. Also, for an inter-cluster iteration, the normalized local model parameter vector is $\bar{\mathbf{w}}_{\mathbf{y}}^{\mathbf{x}} = \frac{\mathbf{w}_{\mathbf{y}}^{\mathbf{x}} - \mu_{\mathbf{w},\mathbf{x}}}{\sigma_{\mathbf{w},\mathbf{x}}}$. Then, at each device \mathbf{y} in the cluster \mathbf{x} , the normalized vector $\bar{\mathbf{g}}_{\mathbf{y}}^{\mathbf{x}}$ or $\bar{\mathbf{w}}_{\mathbf{y}}^{\mathbf{x}}$ is analog modulated and transmitted as $p_{\mathbf{y}}^{\mathbf{x}}\bar{\mathbf{g}}_{\mathbf{y}}^{\mathbf{x}}$ or $p_{\mathbf{y}}^{\mathbf{x}}\bar{\mathbf{w}}_{\mathbf{y}}^{\mathbf{x}}$ simultaneously with other devices in all the clusters, where $|p_{\mathbf{y}}^{\mathbf{x}}|^2$ denotes the transmission power. Thus, the received signal at a server located at \mathbf{z} is

$$\mathbf{v}_{\mathbf{u}}^{\mathbf{z}} = \sum_{\mathbf{x} \in \Phi_p} \sum_{\mathbf{y} \in \mathcal{N}^{\mathbf{x}}} p_{\mathbf{y}}^{\mathbf{x}} \|\mathbf{x} + \mathbf{y} - \mathbf{z}\|^{-\frac{\alpha}{2}} f_{\mathbf{y}\mathbf{z}}^{\mathbf{x}} \bar{\mathbf{s}}_{\mathbf{y}}^{\mathbf{x}} + \mathbf{n}_{\mathbf{u}}^{\mathbf{z}}, \quad \bar{\mathbf{s}}_{\mathbf{y}}^{\mathbf{x}} = \{\bar{\mathbf{g}}_{\mathbf{y}}^{\mathbf{x}}, \bar{\mathbf{w}}_{\mathbf{y}}^{\mathbf{x}}\}, \quad (10)$$

where $\mathbf{n}_{\mathbf{u}}^{\mathbf{z}} \in \mathbb{C}$ is the Gaussian uplink noise with zero mean and variance $\sigma_{\mathbf{n}}^2$.

Each device $\mathbf{y} \in \mathcal{N}^{\mathbf{x}}$ of cluster \mathbf{x} follows a truncated power allocation [18] as

$$p_{\mathbf{y}}^{\mathbf{x}} = \begin{cases} \frac{\sqrt{\rho}}{\|\mathbf{y}\|^{-\frac{\alpha}{2}} f_{\mathbf{y}\mathbf{x}}^{\mathbf{x}}} & |f_{\mathbf{y}\mathbf{x}}^{\mathbf{x}}|^2 \geq \text{th}_1, \\ 0 & |f_{\mathbf{y}\mathbf{x}}^{\mathbf{x}}|^2 < \text{th}_1, \end{cases} \quad (11)$$

where ρ is the power allocation parameter and th_1 is a threshold. We assume that the device knows this channel, the uplink channel to its server. In (11), devices with deep fades do not transmit but the channel pathloss is not included in the conditions. This allows a fair deployment of devices in the learning process, where even devices with high pathloss participate, and thus data diversity is fully utilized [18], [19].

In (11), to meet a maximum average power $P_{\mathbf{u}}$ in each device, we have

$$\begin{aligned} \mathbb{E}\{|p_{\mathbf{y}}^{\mathbf{x}}|^2\} &= \mathbb{E}\left\{\frac{\rho}{\|\mathbf{y}\|^{-\alpha} |f_{\mathbf{y}\mathbf{x}}^{\mathbf{x}}|^2}\right\} = \rho \mathbb{E}\left\{\frac{1}{|f_{\mathbf{y}\mathbf{x}}^{\mathbf{x}}|^2} \mid |f_{\mathbf{y}\mathbf{x}}^{\mathbf{x}}|^2 > \text{th}_1\right\} \mathbb{E}\{\|\mathbf{y}\|^{-\alpha}\} = \rho \text{Ei}(\text{th}_1) \int_{r_0}^R \frac{2y^{1+\alpha}}{R^2 - r_0^2} dy \\ &= \frac{2\rho}{2+\alpha} \text{Ei}(\text{th}_1) \frac{R^{\alpha+2} - r_0^{\alpha+2}}{R^2 - r_0^2} \leq P_{\mathbf{u}}, \end{aligned} \quad (12)$$

where Ei is the exponential integral function defined as $\text{Ei}(x) = \int_x^{\infty} \frac{e^{-t}}{t} dt$. Thus, ρ for all the devices can be selected as

$$\rho = \frac{(2+\alpha)(R^2 - r_0^2)}{2\text{Ei}(\text{th}_1)(R^{\alpha+2} - r_0^{\alpha+2})} P_{\mathbf{u}}. \quad (13)$$

Also, in each time slot, active devices in the cluster \mathbf{x} are given by

$$\mathcal{A}^{\mathbf{x}} = \{\mathbf{y} \in \mathcal{N}^{\mathbf{x}} : |f_{\mathbf{y}\mathbf{x}}^{\mathbf{x}}| \geq \text{th}_1\}, \quad (14)$$

whose cardinality $|\mathcal{A}^x|$ has the binomial distribution with probability $\mathbb{P}\{|f_{yx}^x| \geq \text{th}_1\} = e^{-\text{th}_1}$ and $|\mathcal{A}^x|, \forall \mathbf{x}$ are independent.

B. Downlink for intra-cluster iteration

As $\mathbb{E}\{\mathbf{v}_u^x\} = \mathbf{0}, \forall \mathbf{x}$, each server at a location $\mathbf{x} \in \Phi_p$ normalizes its received signal \mathbf{v}_u^x with its variance, which is $\mathbb{E}\{\|\mathbf{v}_u^o\|^2\}^2$, as $\frac{\mathbf{v}_u^x}{\sqrt{\mathbb{E}\{\|\mathbf{v}_u^o\|^2\}}}$. Then, all the servers transmit the normalized signals simultaneously. Therefore, the received signal at a representative device at \mathbf{y}_0 in the representative cluster \mathbf{o} ³ is

$$\mathbf{v}_{\mathbf{y}_0}^o = \sum_{\mathbf{x} \in \Phi_p} \sqrt{\frac{P_d}{\mathbb{E}\{\|\mathbf{v}_u^o\|^2\}}} \|\mathbf{x} + \mathbf{y}_0\|^{-\frac{\alpha}{2}} f_{yx}^x \mathbf{v}_u^x + \mathbf{n}_d, \quad (15)$$

where P_d is the transmission power constraint of the servers, and $\mathbf{n}_d \in \mathbb{C}$ is the Gaussian downlink noise with zero mean and variance σ_n^2 . From (10) and from the assumption of the MCP-H network topology, each server \mathbf{x} obtains $\mathbb{E}\{\|\mathbf{v}_u^o\|^2\}$ as

$$\begin{aligned} \mathbb{E}\{\|\mathbf{v}_u^o\|^2\} &= \rho \mathbb{E} \left\{ \sum_{\mathbf{x} \in \Phi_p} \sum_{\mathbf{y} \in \mathcal{N}^x} \mathbb{1}(|f_{yx}^x| > \text{th}_1) \frac{\|\mathbf{x} + \mathbf{y}\|^{-\alpha}}{\|\mathbf{y}\|^{-\alpha}} \left| \frac{f_{y\mathbf{o}}^x}{f_{yx}^x} \right|^2 \right\} + \sigma_n^2 = \\ &\rho \mathbb{E} \left\{ \sum_{\mathbf{x} \in \Phi_p} \sum_{\mathbf{y} \in \mathcal{N}^x} \mathbb{1}(|f_{yx}^x| > \text{th}_1) \mathbb{E} \left\{ \frac{|f_{y\mathbf{o}}^x|^2}{|f_{yx}^x|^2} \mid |f_{yx}^x| > \text{th}_1 \right\} \frac{(\|\mathbf{x}\|^2 + \|\mathbf{y}\|^2 - 2\|\mathbf{x}\|\|\mathbf{y}\|\cos(\theta_{xy}))^{-\frac{\alpha}{2}}}{\|\mathbf{y}\|^{-\alpha}} \right\} \\ &+ \sigma_n^2 = \rho \text{Ei}(\text{th}_1) \mathbb{E} \left\{ \sum_{\mathbf{x} \in \Phi_p} \sum_{m=1}^M \binom{M}{m} e^{-\text{th}_1 m} (1 - e^{-\text{th}_1})^{M-m} m \right. \\ &\times \left. \int_0^\infty \left(1 + \frac{\|\mathbf{x}\|^2}{y^2} - 2 \frac{\|\mathbf{x}\|}{y} \cos(\theta_{xy}) \right)^{-\frac{\alpha}{2}} f_{\|\mathbf{y}\|}(y) dy \right\} + \sigma_n^2 \\ &\stackrel{(a)}{=} \rho \text{Ei}(\text{th}_1) \times M e^{-\text{th}_1} \times \lambda_p \int_0^\infty \int_0^{2\pi} \int_0^\infty \left(1 + \frac{x^2}{y^2} - 2 \frac{x}{y} \cos(\theta) \right)^{-\frac{\alpha}{2}} f_{\|\mathbf{y}\|}(y) x dy d\theta dx + \sigma_n^2 \\ &\stackrel{(b)}{=} \frac{2M\rho\lambda_p \text{Ei}(\text{th}_1) e^{-\text{th}_1}}{R^2 - r_0^2} \int_{2r_0}^\infty \int_0^{2\pi} \int_{r_0}^R y \left(1 + \frac{x^2}{y^2} - 2 \frac{x}{y} \cos(\theta) \right)^{-\frac{\alpha}{2}} x dy d\theta dx + \sigma_n^2, \quad (16) \end{aligned}$$

where we replaced $\mathbb{E}\{\|\mathbf{g}_y^x\|^2\} = 1$ and $\mathbb{E}\left\{\frac{|f_{y\mathbf{o}}^x|^2}{|f_{yx}^x|^2} \mid |f_{yx}^x| > \text{th}_1\right\} = \mathbb{E}\{|f_{y\mathbf{o}}^x|^2\} \mathbb{E}\left\{\frac{1}{|f_{yx}^x|^2} \mid |f_{yx}^x| > \text{th}_1\right\} = \text{Ei}(\text{th}_1)$. Also, (a) comes from the Campbell's theorem [25] and (b) is due to the fact that edge servers have at least $2r_0$ distance from each other.

²Due to the symmetry of the network, we have $\mathbb{E}\{\|\mathbf{v}_u^x\|^2\} = \mathbb{E}\{\|\mathbf{v}_u^o\|^2\}, \forall \mathbf{x}$.

³The locations of the representative device and cluster can be anywhere in \mathbb{R}^2 . The origin \mathbf{o} and \mathbf{y}_0 are relatively determined in a coordinate system.

Denormalizing its received signal, the representative device estimates the intra-cluster gradient (6) as

$$\mathbf{g}_{y_0}^o = \frac{\sigma_{g,o} \mathbf{v}_{d_{y_0}}^o}{\sqrt{\rho} \sqrt{\frac{P_d}{\mathbb{E}\{\|\mathbf{v}_u^o\|^2\}} |f^o| \|\mathbf{y}_0\|^{-\frac{\alpha}{2}}}} + \mu_{g,o}, \quad (17)$$

where it is assumed that each device knows its downlink channel from its server and $(\sigma_{g,o}^2, \mu_{g,o})$ is the variance and mean of gradient data over the devices in the representative cluster.

By replacing (10) in (15) and expanding the result, (17) can be rewritten as

$$\mathbf{g}_{y_0}^o = \frac{1}{|\mathcal{A}^o|} \sum_{y \in \mathcal{A}^o} \mathbf{g}_y^o + \frac{\epsilon_u^o}{|\mathcal{A}^o|} + \frac{\epsilon_{d_{y_0}}^o}{|\mathcal{A}^o|}, \quad (18)$$

where ϵ_u^o is the intra-cluster uplink error given by

$$\begin{aligned} \epsilon_u^o &= \frac{\sigma_{g,o}}{\sqrt{\rho}} \sum_{x \in \Phi_p} \sum_{y \in \mathcal{N}^x} \mathbb{1}(|f_{yx}^x|^2 > \text{th}_1) \frac{\sqrt{\rho}}{\|\mathbf{y}\|^{-\frac{\alpha}{2}} f_{yx}^x} \|\mathbf{x} + \mathbf{y}\|^{-\frac{\alpha}{2}} f_{y_0}^x \bar{\mathbf{g}}_y^x + \frac{\sigma_{g,o}}{\sqrt{\rho}} \mathbf{n}_u^o \\ &= \sigma_{g,o} \sum_{x \in \Phi_p} \sum_{y \in \mathcal{N}^x} \mathbb{1}(|f_{yx}^x|^2 > \text{th}_1) \frac{\|\mathbf{x} + \mathbf{y}\|^{-\frac{\alpha}{2}} f_{y_0}^x}{\|\mathbf{y}\|^{-\frac{\alpha}{2}} f_{yx}^x} \bar{\mathbf{g}}_y^x + \frac{\sigma_{g,o}}{\sqrt{\rho}} \mathbf{n}_u^o, \end{aligned} \quad (19)$$

and the intra-cluster downlink error $\epsilon_{d_{y_0}}^o$ is

$$\epsilon_{d_{y_0}}^o = \frac{\sigma_{g,o}}{\sqrt{\rho} \sqrt{\frac{P_d}{\mathbb{E}\{\|\mathbf{v}_u^o\|^2\}} |f^o| \|\mathbf{y}_0\|^{-\frac{\alpha}{2}}}} \sum_{x \in \Phi_p} \sqrt{\frac{P_d}{\mathbb{E}\{\|\mathbf{v}_u^o\|^2\}}} \|\mathbf{x} + \mathbf{y}_0\|^{-\frac{\alpha}{2}} f^x \mathbf{v}_u^x + \frac{\sigma_{g,o} \mathbf{n}_d}{\sqrt{\rho} \sqrt{\frac{P_d}{\mathbb{E}\{\|\mathbf{v}_u^o\|^2\}} |f^o| \|\mathbf{y}_0\|^{-\frac{\alpha}{2}}}}. \quad (20)$$

C. Downlink for inter-cluster iteration

The core server sums and redistributes the signals received from any set of collaborating edge servers. Consider C_x collaborating clusters having the same learning task with a cluster \mathbf{x} , denoted as the set \mathcal{C}_x . Then, the sum of received signals of the clusters in \mathcal{C}_x , i.e., $\sum_{z \in \mathcal{C}_x} \mathbf{v}_u^z$, is normalized with its variance, which is $C_x \mathbb{E}\{\|\mathbf{v}_u^o\|^2\}$, as $\frac{\sum_{z \in \mathcal{C}_x} \mathbf{v}_u^z}{\sqrt{C_x \mathbb{E}\{\|\mathbf{v}_u^o\|^2\}}}$. Then, the result is simultaneously transmitted from the servers of the clusters in \mathcal{C}_x to their devices. Therefore, the received signal at the representative device is

$$\mathbf{v}_{d_{y_0}} = \sum_{x \in \Phi_p} \sqrt{\frac{P_d}{C_x \mathbb{E}\{\|\mathbf{v}_u^o\|^2\}}} \|\mathbf{x} + \mathbf{y}_0\|^{-\frac{\alpha}{2}} f^x \sum_{z \in \mathcal{C}_x} \mathbf{v}_u^z + \mathbf{n}_d. \quad (21)$$

Then, the representative device can estimate the inter-cluster model parameter vector as

$$\mathbf{w}_{y_0}^o = \frac{\sigma_{w,o} \mathbf{v}_{d_{y_0}}}{\sqrt{\rho} \sqrt{\frac{P_d}{C \mathbb{E}\{\|\mathbf{v}_u^o\|^2\}} |f^o| \|\mathbf{y}_0\|^{-\frac{\alpha}{2}} |\mathcal{A}|}} + \mu_{w,o}, \quad (22)$$

where $|\mathcal{A}| = \sum_{\mathbf{x} \in \mathcal{C}} |\mathcal{A}^{\mathbf{x}}|$ and $(\sigma_{\mathbf{w},\mathbf{o}}^2, \mu_{\mathbf{w},\mathbf{o}})$ is the variance and mean of model data over the devices in the representative cluster.

After replacing (10) in (21), (22) can be expanded as

$$\mathbf{w}_{y_0}^{\mathbf{o}} = \frac{1}{|\mathcal{A}|} \sum_{\mathbf{x} \in \mathcal{C}} \sum_{\mathbf{y} \in \mathcal{A}^{\mathbf{x}}} \mathbf{w}_{\mathbf{y}}^{\mathbf{x}} + \frac{\epsilon_{\mathbf{u}}}{|\mathcal{A}|} + \frac{\epsilon_{d_{y_0}}}{|\mathcal{A}|}, \quad (23)$$

where $\epsilon_{\mathbf{u}}$ is the inter-cluster uplink error as

$$\epsilon_{\mathbf{u}} = \sigma_{\mathbf{w},\mathbf{o}} \sum_{\mathbf{z} \in \mathcal{C}} \sum_{\mathbf{x} \in \Phi_{\mathbf{p}}} \sum_{\mathbf{y} \in \mathcal{N}^{\mathbf{x}}} \mathbb{1}(|f_{\mathbf{y}\mathbf{x}}^{\mathbf{x}}|^2 > \text{th}_1) \frac{\|\mathbf{x} + \mathbf{y} - \mathbf{z}\|^{-\frac{\alpha}{2}} f_{\mathbf{y}\mathbf{z}}^{\mathbf{x}}}{\|\mathbf{y}\|^{-\frac{\alpha}{2}} f_{\mathbf{y}\mathbf{x}}^{\mathbf{x}}} \bar{\mathbf{w}}_{\mathbf{y}}^{\mathbf{x}} + \frac{\sigma_{\mathbf{w},\mathbf{o}}}{\sqrt{\rho}} \sum_{\mathbf{z} \in \mathcal{C}} \mathbf{n}_{\mathbf{u}}^{\mathbf{z}}, \quad (24)$$

and the inter-cluster downlink error $\epsilon_{d_{y_0}}$ is

$$\begin{aligned} \epsilon_{d_{y_0}} &= \frac{\sigma_{\mathbf{w},\mathbf{o}}}{\sqrt{\rho} \sqrt{\frac{P_d}{C_{\mathbf{x}} \mathbb{E}\{\|\mathbf{v}_{\mathbf{u}}^{\mathbf{o}}\|^2\}}}} \sum_{\mathbf{x} \in \Phi_{\mathbf{p}}} \sqrt{\frac{P_d}{C_{\mathbf{x}} \mathbb{E}\{\|\mathbf{v}_{\mathbf{u}}^{\mathbf{o}}\|^2\}}} \|\mathbf{x} + \mathbf{y}_0\|^{-\frac{\alpha}{2}} f^{\mathbf{x}} \sum_{\mathbf{z} \in \mathcal{C}_{\mathbf{x}}} \mathbf{v}_{\mathbf{u}}^{\mathbf{z}} \\ &+ \frac{\sigma_{\mathbf{w},\mathbf{o}} \mathbf{n}_{\mathbf{d}}}{\sqrt{\rho} \sqrt{\frac{P_d}{C_{\mathbf{x}} \mathbb{E}\{\|\mathbf{v}_{\mathbf{u}}^{\mathbf{o}}\|^2\}}} |f^{\mathbf{o}}| \|\mathbf{y}_0\|^{-\frac{\alpha}{2}}}. \end{aligned} \quad (25)$$

Note in the intra- and inter-cluster iterations, the uplink error is due to the interference of devices in the uplink and the downlink error comes from the interference of edge servers in the downlink. Also, they include the effect of simultaneous transmissions of all the clusters regardless of their learning tasks.

According to the uplink and downlink schemes, the expected latency in completing the MultiAirFed algorithm is obtained as

$$T_{\text{L}} = T \times (t_{\text{BH}} + 2t_{\text{BC}} + \tau \times (t_{\text{CM}} + 2t_{\text{BC}})), \quad (26)$$

where t_{CM} is the local computation latency of each device given by [33]

$$t_{\text{CM}} = \frac{cN_{\text{b}}}{f}, \quad (27)$$

where c is the number of CPU cycles required for computing one sample data, f is the CPU cycle frequency, and N_{b} is the size of data involved in the local update. In (26), t_{BC} is the time needed for uplink or downlink transmission of d model or gradient parameters as [19]

$$t_{\text{BC}} = \frac{d}{W}, \quad (28)$$

where a total bandwidth of W is assumed. Also, $t_{\text{BH}} \gg t_{\text{BC}}$ denotes the backhaul latency for the inter-cluster process. As observed from (26), the latency is independent of the number of clusters and devices.

V. CONVERGENCE ANALYSIS

Now, according to the estimations in (18) and (23), we present the convergence analysis of MultiAirFed in terms of the optimality gap in the following theorem, under the following common assumptions in the literature [8], [20], [21], [23], [24]:

Assumption 1 (Lipschitz-Continuous Gradient): The gradient of loss function $F(\mathbf{w})$ in (3) is Lipschitz continuous with a non-negative constant $L > 0$. It means that for any model vectors \mathbf{w}_1 and \mathbf{w}_2 , we have

$$F(\mathbf{w}_2) \leq F(\mathbf{w}_1) + \nabla F(\mathbf{w}_1)^T(\mathbf{w}_2 - \mathbf{w}_1) + \frac{L}{2}\|\mathbf{w}_2 - \mathbf{w}_1\|^2, \quad (29)$$

and

$$\|\nabla F(\mathbf{w}_2) - \nabla F(\mathbf{w}_1)\| \leq L\|\mathbf{w}_2 - \mathbf{w}_1\|. \quad (30)$$

Assumption 2 (Variance Bound): The local gradient estimate \mathbf{g} at a device is an unbiased estimate of the ground-true gradient $\nabla F(\mathbf{w})$ with bounded variance

$$\mathbb{E}\{\|\mathbf{g} - \nabla F(\mathbf{w})\|^2\} \leq \frac{\sigma^2}{B}, \quad (31)$$

where B is the mini-batch data size.

Assumption 3 (Polyak-Lojasiewicz Inequality): Consider $F^* = F(\mathbf{w}^*)$ from the problem (4). There is a constant $\delta \geq 0$ such that the following condition is satisfied.

$$\|\nabla F(\mathbf{w})\|^2 \geq 2\delta(F(\mathbf{w}) - F^*). \quad (32)$$

Note that the inequality (32) is broader than the strong convexity assumption [32].

Theorem 1: Consider a fixed learning rate μ satisfying

$$1 - \frac{L^2\mu^2\tau(\tau-1)}{2} - L\mu\tau \geq 0. \quad (33)$$

Then, the following optimality gap holds for the local learning model of any representative device $\mathbf{y}_0 \in \mathcal{N}^\circ$,

$$\begin{aligned} \mathbb{E}\{F(\mathbf{w}_{\mathbf{y}_0,0,T}^\circ)\} - F^* &\leq (1 - \mu\tau\delta)^T \left(F(\mathbf{w}_{\mathbf{y}_0,0,0}^\circ) - F^* \right) + \frac{1 - (1 - \mu\tau\delta)^T}{\mu\tau\delta} \times \\ &\left[\frac{L^2\mu^3}{4} \frac{\sigma^2}{B} \tau(\tau-1) \mathbb{E}\left\{ \frac{1}{|\mathcal{A}^\circ|} \right\} + \frac{L\mu^2}{2} \frac{\sigma^2}{B} \tau \mathbb{E}\left\{ \frac{1}{|\mathcal{A}^\circ|} \right\} \mathbb{E}\left\{ \sum_{\mathbf{x} \in \mathcal{C}} \frac{|\mathcal{A}^{\mathbf{x}}|^2}{|\mathcal{A}|^2} \right\} \right] \\ &+ \mathbb{E}\left\{ \frac{1}{|\mathcal{A}^\circ|^2} \right\} \left(\frac{L^2\mu^3}{4} \tau(\tau-1) + \frac{L\mu^2}{2} \tau \mathbb{E}\left\{ \sum_{\mathbf{x} \in \mathcal{C}} \frac{|\mathcal{A}^{\mathbf{x}}|^2}{|\mathcal{A}|^2} \right\} \right) \mathbb{E}\{\|\boldsymbol{\epsilon}_u^\circ\|^2\} \\ &+ \mathbb{E}\left\{ \frac{1}{|\mathcal{A}^\circ|^2} \right\} \left(\frac{L^2\mu^3}{4} \tau(\tau-1) + \frac{L\mu^2}{2} \tau \mathbb{E}\left\{ \frac{1}{|\mathcal{A}|} \right\} \right) \mathbb{E}\{\|\boldsymbol{\epsilon}_{d_{\mathbf{y}_0}}^\circ\|^2\} \end{aligned}$$

$$\begin{aligned}
& + \frac{L}{2} \mathbb{E} \left\{ \frac{1}{|\mathcal{A}|^2} \right\} \mathbb{E} \{ \|\epsilon_u\|^2 \} \\
& + \mathbb{E} \left\{ \frac{1}{|\mathcal{A}|^2} \right\} \left(L^2 \mu \tau + \frac{L}{2} \mathbb{E} \left\{ \frac{1}{|\mathcal{A}|} \right\} + L \right) \mathbb{E} \{ \|\epsilon_{d_{y_0}}\|^2 \}.
\end{aligned} \tag{34}$$

Proof: See Appendix A. ■

Considering the error term in the bound, the first two parts reflect the gradient estimation errors. These are followed by the effects of the intra- and inter-cluster uplink and downlink errors. The scaling factors of the error terms depend on the learning parameters and on the device selection, while the error terms depend on the interference, determined by network topology, the wireless environment and the power control.

To obtain the bound for the proposed clustered scheme in Section IV, we characterize the expected terms on the number of active devices $\mathbb{E} \left\{ \frac{1}{|\mathcal{A}^\circ|} \right\}$, $\mathbb{E} \left\{ \frac{1}{|\mathcal{A}^\circ|^2} \right\}$, $\mathbb{E} \left\{ \frac{1}{|\mathcal{A}|} \right\}$, $\mathbb{E} \left\{ \frac{1}{|\mathcal{A}|^2} \right\}$, and $\mathbb{E} \left\{ \sum_{\mathbf{x} \in \mathcal{C}} \frac{|\mathcal{A}^{\mathbf{x}}|^2}{|\mathcal{A}|^2} \right\}$, and the expected terms on the uplink and downlink errors $\mathbb{E} \{ \|\epsilon_u^\circ\|^2 \}$, $\mathbb{E} \{ \|\epsilon_{d_{y_0}}^\circ\|^2 \}$, $\mathbb{E} \{ \|\epsilon_u\|^2 \}$, and $\mathbb{E} \{ \|\epsilon_{d_{y_0}}\|^2 \}$ as follows.

Due to the facts that $|\mathcal{A}^{\mathbf{x}}| \sim \text{Binomial}(M, e^{-\text{th}_1})$, $\forall \mathbf{x}$, $|\mathcal{A}| \sim \text{Binomial}(CM, e^{-\text{th}_1})$, and there is at least one active device in each cluster, the expected terms on the number of active devices are computed as

$$\begin{aligned}
\mathbb{E} \left\{ \frac{1}{|\mathcal{A}^\circ|} \middle| |\mathcal{A}^\circ| > 0 \right\} &= \frac{\mathbb{E} \left\{ \frac{1}{|\mathcal{A}^\circ|} \text{ and } |\mathcal{A}^\circ| > 0 \right\}}{\mathbb{P} \{ |\mathcal{A}^\circ| > 0 \}} = \sum_{m=1}^M \frac{1}{m} \frac{\binom{M}{m} e^{-\text{th}_1 m} (1 - e^{-\text{th}_1})^{M-m}}{1 - (1 - e^{-\text{th}_1})^M} \\
&= \frac{(1 - e^{-\text{th}_1})^M}{1 - (1 - e^{-\text{th}_1})^M} \sum_{m=1}^M \binom{M}{m} \frac{1}{m} \left(\frac{e^{-\text{th}_1}}{1 - e^{-\text{th}_1}} \right)^m,
\end{aligned} \tag{35}$$

$$\mathbb{E} \left\{ \frac{1}{|\mathcal{A}^\circ|^2} \middle| |\mathcal{A}^\circ| > 0 \right\} = \frac{(1 - e^{-\text{th}_1})^M}{1 - (1 - e^{-\text{th}_1})^M} \sum_{m=1}^M \binom{M}{m} \frac{1}{m^2} \left(\frac{e^{-\text{th}_1}}{1 - e^{-\text{th}_1}} \right)^m, \tag{36}$$

$$\begin{aligned}
\mathbb{E} \left\{ \frac{1}{|\mathcal{A}|} \middle| |\mathcal{A}^{\mathbf{x}}| > 0, \forall \mathbf{x} \right\} &= \frac{\mathbb{E} \left\{ \frac{1}{|\mathcal{A}|} \text{ and } |\mathcal{A}| > C \right\}}{\prod_{\mathbf{x} \in \mathcal{C}} \mathbb{P} \{ |\mathcal{A}^{\mathbf{x}}| > 0 \}} = \sum_{m=C}^{CM} \frac{1}{m} \frac{\binom{CM}{m} e^{-\text{th}_1 m} (1 - e^{-\text{th}_1})^{CM-m}}{(1 - (1 - e^{-\text{th}_1})^M)^C} \\
&= \left(\frac{(1 - e^{-\text{th}_1})^M}{1 - (1 - e^{-\text{th}_1})^M} \right)^C \sum_{m=C}^{CM} \binom{CM}{m} \frac{1}{m} \left(\frac{e^{-\text{th}_1}}{1 - e^{-\text{th}_1}} \right)^m,
\end{aligned} \tag{37}$$

$$\mathbb{E} \left\{ \frac{1}{|\mathcal{A}|^2} \middle| |\mathcal{A}^{\mathbf{x}}| > 0, \forall \mathbf{x} \right\} = \left(\frac{(1 - e^{-\text{th}_1})^M}{1 - (1 - e^{-\text{th}_1})^M} \right)^C \sum_{m=C}^{CM} \binom{CM}{m} \frac{1}{m^2} \left(\frac{e^{-\text{th}_1}}{1 - e^{-\text{th}_1}} \right)^m, \tag{38}$$

$$\mathbb{E} \left\{ \sum_{\mathbf{x} \in \mathcal{C}} \frac{|\mathcal{A}^{\mathbf{x}}|^2}{|\mathcal{A}|^2} \mid |\mathcal{A}^{\mathbf{x}}| > 0, \forall \mathbf{x} \right\} = \left(\frac{(1 - e^{-\text{th}_1})^M}{1 - (1 - e^{-\text{th}_1})^M} \right)^C \times$$

$$\sum_{m=C}^{MC} \binom{CM}{m} \frac{\sum_{\{(m_1, \dots, m_C) \mid \sum_{c=1}^C m_c = m\}} \sum_{c=1}^C m_c^2}{m^2} \left(\frac{e^{-\text{th}_1}}{1 - e^{-\text{th}_1}} \right)^m.$$
(39)

Then, for the expected terms on the uplink and downlink errors: from (10) and (19), $\mathbb{E} \{ \|\epsilon_{\mathbf{u}}^{\circ}\|^2 \} = \frac{\sigma_{\mathbf{g}, \mathbf{o}}^2}{\rho} \mathbb{E} \{ \|\mathbf{v}_{\mathbf{u}}^{\circ}\|^2 \}$, and due to the MCP-H network topology and from (20)

$$\mathbb{E} \left\{ \|\epsilon_{\mathbf{d}_{\mathbf{y}_0}}^{\circ}\|^2 \right\} = \mathbb{E} \left\{ \frac{\sigma_{\mathbf{g}, \mathbf{o}}^2}{\rho \frac{P_d}{\mathbb{E}\{\|\mathbf{v}_{\mathbf{u}}^{\circ}\|^2\}}} |f^{\circ}|^2 \|\mathbf{y}_0\|^{-\alpha} \sum_{\mathbf{x} \in \Phi_p} P_d \|\mathbf{x} + \mathbf{y}_0\|^{-\alpha} |f^{\mathbf{x}}|^2 \right\} + \mathbb{E} \left\{ \frac{\sigma_{\mathbf{g}, \mathbf{o}}^2 \sigma_n^2}{\rho \frac{P_d}{\mathbb{E}\{\|\mathbf{v}_{\mathbf{u}}^{\circ}\|^2\}}} |f^{\circ}|^2 \|\mathbf{y}_0\|^{-\alpha} \right\}$$

$$\stackrel{(c)}{=} \frac{\sigma_{\mathbf{g}, \mathbf{o}}^2}{\rho} \mathbb{E} \{ \|\mathbf{v}_{\mathbf{u}}^{\circ}\|^2 \} \text{Ei}(\text{th}_0) \frac{2}{2 + \alpha} \frac{R^{\alpha+2} - r_0^{\alpha+2}}{R^2 - r_0^2} 2\pi \lambda_p \int_{r_0}^{\infty} x^{1-\alpha} dx + \frac{\sigma_{\mathbf{g}, \mathbf{o}}^2 \sigma_n^2}{\rho P_d} \mathbb{E} \{ \|\mathbf{v}_{\mathbf{u}}^{\circ}\|^2 \} \text{Ei}(\text{th}_0) \frac{2}{2 + \alpha} \times$$

$$\frac{R^{\alpha+2} - r_0^{\alpha+2}}{R^2 - r_0^2} = \frac{2\sigma_{\mathbf{g}, \mathbf{o}}^2 (R^{\alpha+2} - r_0^{\alpha+2})}{\rho(\alpha + 2)(R^2 - r_0^2)} \mathbb{E} \{ \|\mathbf{v}_{\mathbf{u}}^{\circ}\|^2 \} \text{Ei}(\text{th}_0) \left(\frac{2\pi \lambda_p}{(\alpha - 2)r_0^{\alpha-2}} + \frac{\sigma_n^2}{P_d} \right),$$
(40)

where (c) is due to $\mathbb{E} \{ \|\mathbf{y}_0\|^{\alpha} \} = \int_{r_0}^R \frac{2y}{R^2 - r_0^2} y^{\alpha} dy = \frac{2}{2 + \alpha} \frac{R^{\alpha+2} - r_0^{\alpha+2}}{R^2 - r_0^2}$ and the Campbell's theorem. Also, due to the symmetry of the network and the error terms in (19)-(20) and (24)-(25), we have $\mathbb{E} \{ \|\epsilon_{\mathbf{u}}\|^2 \} = C \frac{\sigma_{\mathbf{w}, \mathbf{o}}^2}{\sigma_{\mathbf{g}, \mathbf{o}}^2} \mathbb{E} \{ \|\epsilon_{\mathbf{u}}^{\circ}\|^2 \}$ and $\mathbb{E} \{ \|\epsilon_{\mathbf{d}_{\mathbf{y}_0}}\|^2 \} = C \frac{\sigma_{\mathbf{w}, \mathbf{o}}^2}{\sigma_{\mathbf{g}, \mathbf{o}}^2} \mathbb{E} \{ \|\epsilon_{\mathbf{d}_{\mathbf{y}_0}}^{\circ}\|^2 \}$.

The following remarks and design insights can be concluded from Theorem 1.

Remark 1: The first term of the optimality gap decreases with the number of inter-cluster iterations T , while the second, error term is increasing, approaching a bound.

Remark 2: There is a tradeoff for the optimality gap when th_1 increases. The term $\text{Ei}(\text{th}_1)e^{-\text{th}_1}$ and then the intra-cluster uplink error term $\mathbb{E} \{ \|\epsilon_{\mathbf{u}}^{\circ}\|^2 \}$ decrease, however the term $\mathbb{E} \left\{ \frac{1}{|\mathcal{A}^{\circ}|} \right\}$ in (35) increases. Hence, the impact of threshold th_1 on the convergence in the general case is not evident.

Remark 3: The scaling factors of the intra-cluster uplink and downlink error terms $\mathbb{E} \{ \|\epsilon_{\mathbf{u}}^{\circ}\|^2 \}$ and $\mathbb{E} \left\{ \|\epsilon_{\mathbf{d}_{\mathbf{y}_0}}^{\circ}\|^2 \right\}$ in the optimality gap increase by τ and μ with the rate $\mathcal{O}(\mu^3 \tau^2)$. Also, while the scaling factor of the inter-cluster uplink error term $\mathbb{E} \{ \|\epsilon_{\mathbf{u}}\|^2 \}$ does not change with them, the scaling factor of the inter-cluster downlink error term $\mathbb{E} \{ \|\epsilon_{\mathbf{d}_{\mathbf{y}_0}}\|^2 \}$ increases with the rate $\mathcal{O}(\mu\tau)$. Hence, the intra-cluster error terms grow the optimality gap with τ and μ much faster compared to the inter-cluster error terms.

Remark 4: When $\mu \propto \frac{1}{\tau}$, the optimality gap has the rate $\mathcal{O}(\text{const} + \frac{1}{\tau})$ with τ . Hence, increasing τ decreases the gap.

Remark 5: In the optimality gap, the intra-cluster error terms $\mathbb{E}\{\|\epsilon_u^o\|^2\}$ and $\mathbb{E}\{\|\epsilon_{d_{y_0}}^o\|^2\}$ are directly scaled by the inverse squared of the number of active devices in a single cluster $\mathbb{E}\left\{\frac{1}{|\mathcal{A}^o|^2}\right\}$. Also, the inter-cluster error terms $\mathbb{E}\{\|\epsilon_u\|^2\}$ and $\mathbb{E}\{\|\epsilon_{d_{y_0}}\|^2\}$ are scaled by the inverse squared of the total number of active devices in the collaborating clusters $\mathbb{E}\left\{\frac{1}{|\mathcal{A}|^2}\right\}$. Hence, having higher number of active devices in the learning process can significantly diminish the effect of error terms in the optimality gap.

Remark 6: Increasing the number of collaborating clusters C decreases $\mathbb{E}\left\{\frac{1}{|\mathcal{A}|}\right\}$ and $\mathbb{E}\left\{\frac{1}{|\mathcal{A}|^2}\right\}$ with an order higher than one as in (37) and (38). On the other hand, the inter-cluster error terms $\mathbb{E}\{\|\epsilon_u\|^2\}$ and $\mathbb{E}\{\|\epsilon_{d_{y_0}}\|^2\}$ linearly increase with C . Hence, overallly the optimality gap decreases.

Remark 7: The scaling factor, or the effect on the optimality gap, of the intra-cluster uplink error term $\mathbb{E}\{\|\epsilon_u^o\|^2\}$ is more than the one for the intra-cluster downlink error term $\mathbb{E}\left\{\|\epsilon_{d_{y_0}}^o\|^2\right\}$. That is due to the fact that $\sum_{x \in C} |\mathcal{A}^x|^2 > |\mathcal{A}|$ and hence $\frac{L^2\mu^3}{4}\tau(\tau-1) + \frac{L\mu^2}{2}\tau\mathbb{E}\left\{\sum_{x \in C} \frac{|\mathcal{A}^x|^2}{|\mathcal{A}|^2}\right\} > \frac{L^2\mu^3}{4}\tau(\tau-1) + \frac{L\mu^2}{2}\tau\mathbb{E}\left\{\frac{1}{|\mathcal{A}|}\right\}$. However, for the inter-cluster error terms, the downlink term $\mathbb{E}\{\|\epsilon_{d_{y_0}}\|^2\}$ has higher scaling factor than the uplink term $\mathbb{E}\{\|\epsilon_u\|^2\}$ since the inequality $L^2\mu\tau + \frac{L}{2}\mathbb{E}\left\{\frac{1}{|\mathcal{A}|}\right\} + L > \frac{L}{2}$ holds.

Remark 8: From (16) and (40), the uplink error terms $\mathbb{E}\{\|\epsilon_u^o\|^2\}$ and $\mathbb{E}\{\|\epsilon_u\|^2\}$ and the downlink error terms $\mathbb{E}\left\{\|\epsilon_{d_{y_0}}^o\|^2\right\}$ and $\mathbb{E}\{\|\epsilon_{d_{y_0}}\|^2\}$ linearly and quadratically⁴ increase with the cluster center density λ_p , respectively. Hence, the optimality gap increases with the rate $\mathcal{O}(\lambda_p^2)$.

Remark 9: From (16), the intra- and inter-cluster uplink error terms $\mathbb{E}\{\|\epsilon_u^o\|^2\}$ and $\mathbb{E}\{\|\epsilon_u\|^2\}$ linearly increase with the number of devices per cluster, M . However, from (36) and (38), as $\mathbb{E}\left\{\frac{1}{|\mathcal{A}^o|^2}\right\}$ and $\mathbb{E}\left\{\frac{1}{|\mathcal{A}|^2}\right\}$ decrease with M at orders higher than one and they contribute to all the scaling factors of the error terms, the optimality gap is overallly decreased.

In the following corollaries, we present special cases of Theorem 1. For the single-server case when all edge servers are working independently under different learning tasks, i.e., $C = 1$, we have the next simplified convergence result.

Corollary 1: In the case $C = 1$ and the learning rate

$$1 - \frac{L^2\mu^2\tau(\tau-1)}{2} - L\mu\tau \geq 0, \quad (41)$$

⁴Note that the term $\mathbb{E}\{\|\mathbf{v}_u^o\|^2\}$ in (40) has a linear dependency to λ_p , as given in (16).

the optimality gap for the local learning model of any representative device $\mathbf{y}_0 \in \mathcal{N}^\circ$ is

$$\begin{aligned} \mathbb{E} \{F(\mathbf{w}_{\mathbf{y}_0,0,T}^\circ)\} - F^* &\leq (1 - \mu\tau\delta)^T \left(F(\mathbf{w}_{\mathbf{y}_0,0,0}^\circ) - F^* \right) + \frac{1 - (1 - \mu\tau\delta)^T}{\mu\tau\delta} \times \\ &\left[\frac{L^2\mu^3\sigma^2}{4B} \tau(\tau - 1) \mathbb{E} \left\{ \frac{1}{|\mathcal{A}^\circ|} \right\} + \frac{L\mu^2\sigma^2}{2B} \tau \mathbb{E} \left\{ \frac{1}{|\mathcal{A}^\circ|} \right\} + \left(\frac{L^2\mu^3}{4} \tau(\tau - 1) + \frac{L\mu^2}{2} \tau + \frac{L}{2} \right) \times \right. \\ &\mathbb{E} \left\{ \frac{1}{|\mathcal{A}^\circ|^2} \right\} \mathbb{E} \{ \|\epsilon_{\mathbf{u}}^\circ\|^2 \} + \left(\frac{L^2\mu^3}{4} \tau(\tau - 1) + L^2\mu\tau + L + \left(\frac{L\mu^2\tau}{2} + \frac{L}{2} \right) \mathbb{E} \left\{ \frac{1}{|\mathcal{A}^\circ|} \right\} \right) \times \\ &\left. \mathbb{E} \left\{ \frac{1}{|\mathcal{A}^\circ|^2} \right\} \mathbb{E} \{ \|\epsilon_{\mathbf{d}_{\mathbf{y}_0}}^\circ\|^2 \} \right]. \end{aligned} \quad (42)$$

Proof: It comes from Theorem 1 when $\mathcal{A} = \mathcal{A}^\circ$ and $\mathbb{E} \left\{ \sum_{\mathbf{x} \in \mathcal{C}} \frac{|\mathcal{A}^{\mathbf{x}}|^2}{|\mathcal{A}|^2} \right\} = 1$. \blacksquare

When all the edge servers are collaboratively working under the same task, i.e., $C \rightarrow \infty$, the convergence result is simplified in the next corollary.

Corollary 2: In the case $C \rightarrow \infty$ and the learning rate

$$1 - \frac{L^2\mu^2\tau(\tau - 1)}{2} - L\mu\tau \geq 0, \quad (43)$$

the optimality gap for the local learning model of any representative device $\mathbf{y}_0 \in \mathcal{N}^\circ$ is

$$\begin{aligned} \mathbb{E} \{F(\mathbf{w}_{\mathbf{y}_0,0,T}^\circ)\} - F^* &\leq (1 - \mu\tau\delta)^T \left(F(\mathbf{w}_{\mathbf{y}_0,0,0}^\circ) - F^* \right) + \frac{1 - (1 - \mu\tau\delta)^T}{\mu\tau\delta} \times \\ &\left[\frac{L^2\mu^3\sigma^2}{4B} \tau(\tau - 1) \mathbb{E} \left\{ \frac{1}{|\mathcal{A}^\circ|} \right\} + \mathbb{E} \left\{ \frac{1}{|\mathcal{A}^\circ|^2} \right\} \left(\frac{L^2\mu^3}{4} \tau(\tau - 1) \right) \mathbb{E} \{ \|\epsilon_{\mathbf{u}}^\circ\|^2 \} \right. \\ &\left. + \mathbb{E} \left\{ \frac{1}{|\mathcal{A}^\circ|^2} \right\} \left(\frac{L^2\mu^3}{4} \tau(\tau - 1) \right) \mathbb{E} \{ \|\epsilon_{\mathbf{d}_{\mathbf{y}_0}}^\circ\|^2 \} \right]. \end{aligned} \quad (44)$$

Proof: It comes from Theorem 1 when $\mathbb{E} \left\{ \frac{1}{|\mathcal{A}|} \right\} = 0$ and $\mathbb{E} \left\{ \frac{1}{|\mathcal{A}|^2} \right\} = 0$. Also, $\mathbb{E} \left\{ \sum_{\mathbf{x} \in \mathcal{C}} \frac{|\mathcal{A}^{\mathbf{x}}|^2}{|\mathcal{A}|^2} \right\} = 0$ since $|\mathcal{A}|^2 = \sum_{\mathbf{x} \in \mathcal{C}} |\mathcal{A}^{\mathbf{x}}|^2 + \sum_{\substack{\mathbf{x}, \mathbf{x}' \in \mathcal{C} \\ \mathbf{x} \neq \mathbf{x}'}} 2|\mathcal{A}^{\mathbf{x}}||\mathcal{A}^{\mathbf{x}'}|$ and $\lim_{C \rightarrow \infty} \sum_{\substack{\mathbf{x}, \mathbf{x}' \in \mathcal{C} \\ \mathbf{x} \neq \mathbf{x}'}} 2|\mathcal{A}^{\mathbf{x}}||\mathcal{A}^{\mathbf{x}'}| = \infty$. \blacksquare

Remark 10: Three terms in the optimality gap given in Theorem 1, the two terms of the inter-cluster uplink and downlink errors and the term $\frac{L\mu^2\sigma^2}{2B} \tau \mathbb{E} \left\{ \frac{1}{|\mathcal{A}^\circ|} \right\} \mathbb{E} \left\{ \sum_{\mathbf{x} \in \mathcal{C}} \frac{|\mathcal{A}^{\mathbf{x}}|^2}{|\mathcal{A}|^2} \right\}$, vanish when $C \rightarrow \infty$.

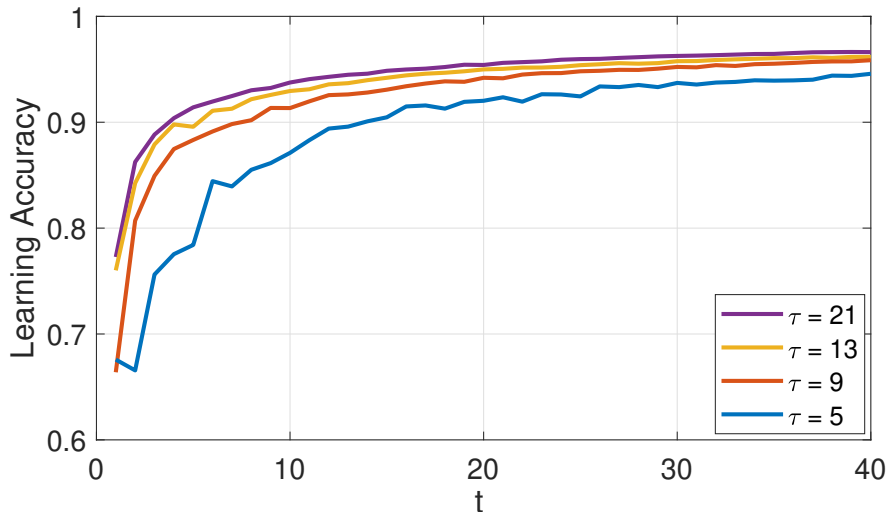
Remark 11: The scaling factors of the intra-cluster error terms $\mathbb{E} \{ \|\epsilon_{\mathbf{u}}^\circ\|^2 \}$ and $\mathbb{E} \{ \|\epsilon_{\mathbf{d}_{\mathbf{y}_0}}^\circ\|^2 \}$ approaches to equal terms when $C \rightarrow \infty$, thus their effect on the convergence will be the same.

VI. EXPERIMENTAL RESULTS

The classification learning task is the handwritten-digit recognition on the standard MNIST dataset [34]. Each sample in MNIST dataset is a 28×28 image. The dataset size for training

TABLE I: Parameter Values

λ_p	r_0	R	μ	C	M	P_u	P_d	$\{th_0, th_1\}$	α	τ	T	W	N_b	$\{c, f\}$
20 Km^{-2}	4 m	30 m	0.01	3	15	1	10	$\{0.1, 0.5\}$	4	6	40	1 MHz	2.5 Mbit	$\{20 \text{ Cycles/bit}, 1 \text{ GHz}\}$

Fig. 2: Learning accuracy as a function of global iterations t .

is 37800 and the dataset for testing has size 4200. The training dataset is divided equally at random over the devices within a cluster. The classifier model is implemented using a 3-layer convolutional neural network (CNN) with 200 hidden units at each layer, which has 199210 trainable parameters. Input of the model is flattened. Also, the ReLU activation function in the hidden layers and softmax in the output layer are used. The performance is measured as the learning accuracy with reference to the test dataset over global inter-cluster iteration count t . Each performance result is evaluated as the average of 10 realization samples to account for random network distributions.

In Fig. 2, the accuracy is shown for different intra-cluster iterations τ . As observed, increasing τ or T improves the learning performance and convergence speed, justifying *Remarks 1* and *4*. Also, the improvement gap is decreased in higher numbers of intra- or inter-cluster iterations. It shows that a minimum number of intra- and inter-cluster iterations can ensure a desirable performance.

The latency T_L given in (26) is plotted in Fig. 3 for different τ when the target learning accuracy 95% is achieved. We assume $t_{BH} = 10t_{BC}$. As observed, the latency is minimized at $\tau = 13$. For higher values, the convergence rate does not increase sufficiently to compensate

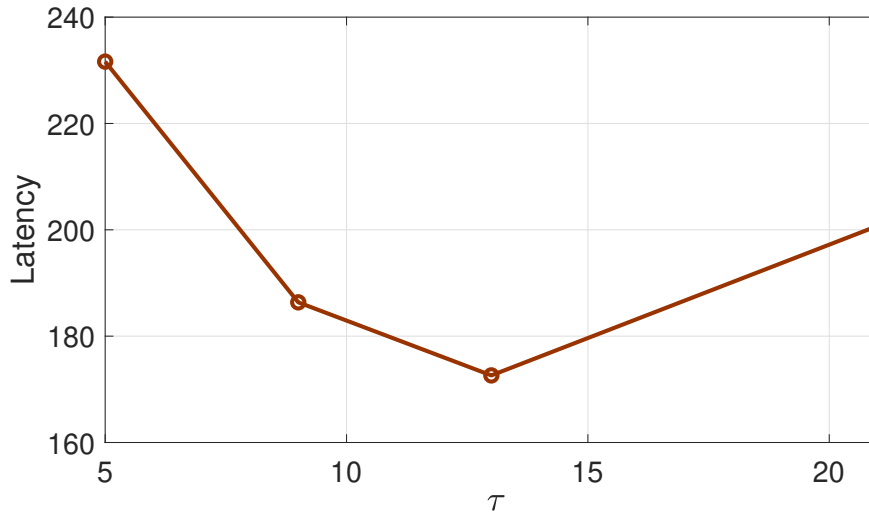


Fig. 3: Latency in seconds as a function of intra-cluster iterations τ .

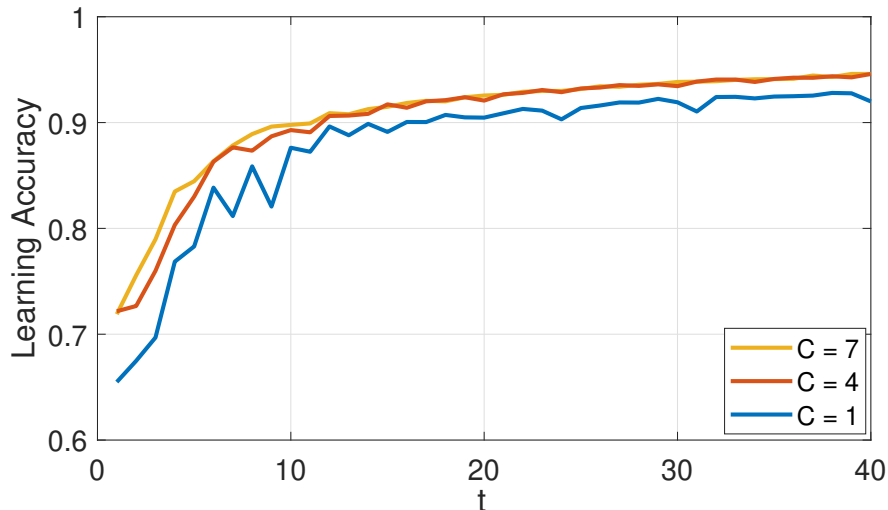


Fig. 4: Learning accuracy as a function of global iterations t .

for the longer time for the intra-cluster iterations.

In Fig. 4, the accuracy for different values of the number of collaborating clusters with the same task is studied. It is observed that the multi-server case can significantly improve the accuracy compared to the single-server case. It justifies *Remark 6*. That is because of accessing a diverse set of intra-cluster learning models and increasing the total active devices in the learning process over different clusters.

In Fig. 5, the accuracy is shown for different numbers of devices M in each cluster. The performance is improved as M increases since the number of active devices that can participate in the learning process increases. It justifies *Remark 9*. However, it is observed that increasing

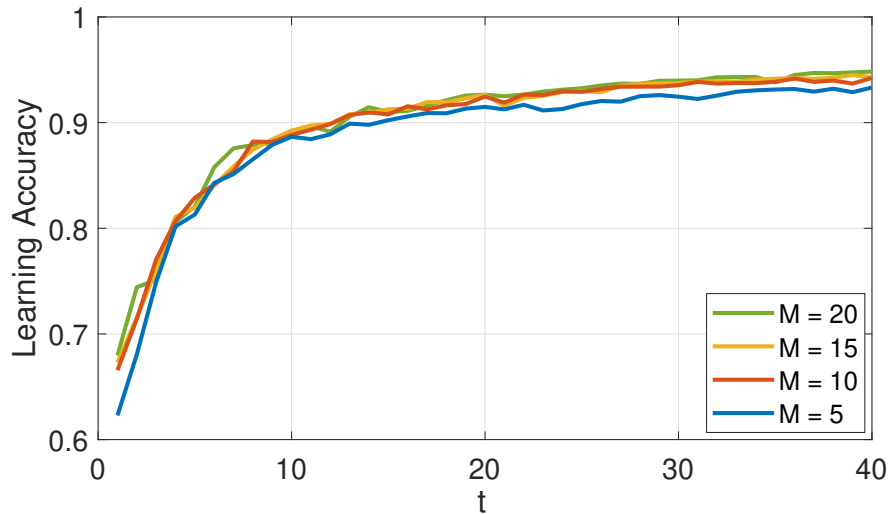


Fig. 5: Learning accuracy as a function of global iterations t .

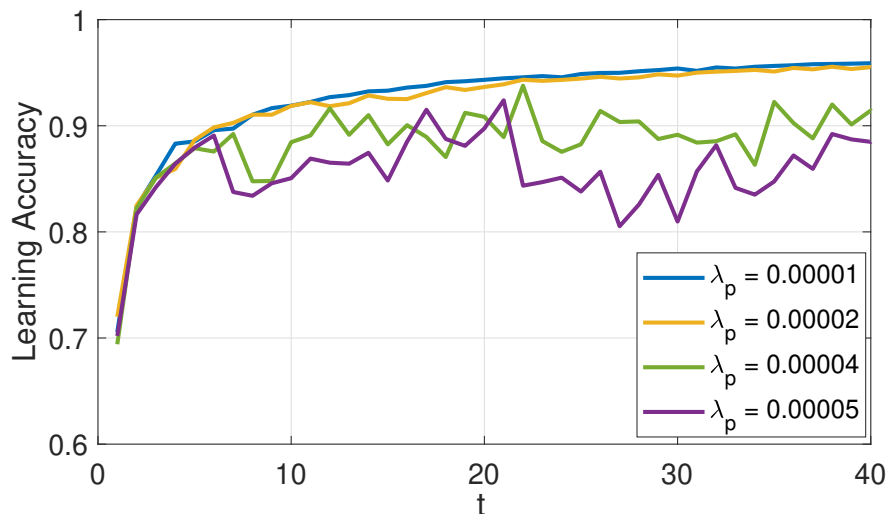


Fig. 6: Learning accuracy as a function of global iterations t .

M does not provide a significant impact. This is because there is a trade-off as M increases. Although desirable active devices in the clusters of interest increase, interfering devices over the network increase.

In Fig. 6, the effect of the cluster center density λ_p is investigated on the accuracy. As observed, the accuracy decreases as λ_p increases. It justifies *Remark 8*. This is due to the increase in the interference. Also, in $\lambda_p \geq 0.00004 \text{ m}^{-2}$, there is a non-smooth behavior. That is because the estimation noises in recovering gradient and model parameters in intra- and inter-cluster iterations can significantly increase, resulting in a deviated gradient for local model updating. However, the average performance is still acceptable.

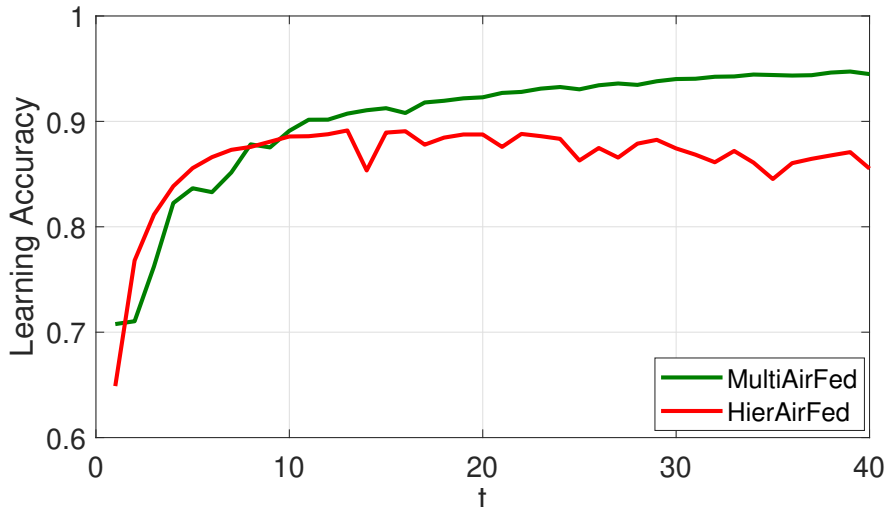


Fig. 7: Learning accuracy as a function of global iterations t .

In Fig. 7, the learning performance of MultiAirFed is compared with the conventional hierarchical FL in [8]–[10] when $\lambda_p = 40 \text{ Km}^{-2}$ and $M = 25$. We name this benchmark HierAirFed. For each intra-cluster iteration in HierAirFed, model parameters are uploaded to the edge servers and the initial state at each local device is synchronized, while in MultiAirFed the gradient is uploaded. HierAirFed is a learning algorithm and does not contain a wireless transmission scheme. Therefore, for a fair comparison, we use the same proposed "clustered" framework as in Section IV for its employments in the proposed wireless setup. As observed, MultiAirFed has a significantly better performance than HierAirFed. That is because the noisy transmission of model parameters over the air leads to deviations in both the initial state and local gradient at the devices. However, when gradients are transmitted, each device can download the aggregated gradient as the required gradient for its update with no local imperfect computations and state deviations. Compared to Fig. 6, it is also observed that increasing M from 15 to 25 provides the smooth behavior for the performance.

VII. CONCLUSIONS

In this paper, we proposed a new two-layer federated learning algorithm that leverages the clustered network architecture and intra- and inter-cluster collaborations for a higher communication-efficiency and learning accuracy. To practically implement the proposed algorithm over wireless distributed systems independent of their scale and with minimum resource requirements, we presented an over-the-air aggregation scheme for the uplink and a bandwidth-limited broadcast

scheme for the downlink under limited transmit powers. Also, to take into account the location correlation between the devices and their respective edge servers, we modeled a setup including clusters of devices as a PCP with the edge servers at the cluster centers. Then, we provided a convergence bound analysis for the proposed algorithm in the setup with special cases including different number of collaborating clusters from 1 to ∞ . Also, we provided experimental results to evaluate the learning accuracy and latency of the proposed algorithm in the setup and confirm the design remarks from the analysis. We also showed that the proposed gradient based hierarchical FL outperforms existing solutions, and the achieved accuracy is high, despite the interference.

APPENDIX A

PROOF OF THEOREM 1

In the proof, we show the index for the intra- and inter-cluster iterations. Then, update of the learning model at global inter-cluster iteration $t + 1$ is represented as

$$\begin{aligned}
\mathbf{w}_{y_0,0,t+1}^o &= \frac{1}{|\mathcal{A}_{\tau,t}|} \sum_{\mathbf{x} \in \mathcal{C}} \sum_{\mathbf{y} \in \mathcal{A}_{\tau,t}^{\mathbf{x}}} \mathbf{w}_{\mathbf{y},\tau,t}^{\mathbf{x}} + \frac{\epsilon_{ut}}{|\mathcal{A}_{\tau,t}|} + \frac{\epsilon_{dy_0,t}}{|\mathcal{A}_{\tau,t}|} \\
&= \frac{1}{|\mathcal{A}_{\tau,t}|} \sum_{\mathbf{x} \in \mathcal{C}} \sum_{\mathbf{y} \in \mathcal{A}_{\tau,t}^{\mathbf{x}}} \left(\mathbf{w}_{\mathbf{y},0,t}^{\mathbf{x}} - \mu_t \sum_{i=0}^{\tau-1} \mathbf{g}_{\mathbf{y},i,t}^{\mathbf{x}} \right) + \frac{\epsilon_{ut}}{|\mathcal{A}_{\tau,t}|} + \frac{\epsilon_{dy_0,t}}{|\mathcal{A}_{\tau,t}|} \\
&= -\frac{\mu_t}{|\mathcal{A}_{\tau,t}|} \sum_{\mathbf{x} \in \mathcal{C}} \sum_{\mathbf{y} \in \mathcal{A}_{\tau,t}^{\mathbf{x}}} \sum_{i=0}^{\tau-1} \mathbf{g}_{\mathbf{y},i,t}^{\mathbf{x}} + \frac{1}{|\mathcal{A}_{\tau,t}|} \sum_{\mathbf{x} \in \mathcal{C}} \sum_{\mathbf{y} \in \mathcal{A}_{\tau,t}^{\mathbf{x}}} \mathbf{w}_{\mathbf{y},0,t}^{\mathbf{x}} + \frac{\epsilon_{ut}}{|\mathcal{A}_{\tau,t}|} + \frac{\epsilon_{dy_0,t}}{|\mathcal{A}_{\tau,t}|} \\
&= -\frac{\mu_t}{|\mathcal{A}_{\tau,t}|} \sum_{\mathbf{x} \in \mathcal{C}} \sum_{\mathbf{y} \in \mathcal{A}_{\tau,t}^{\mathbf{x}}} \sum_{i=0}^{\tau-1} \left(\mathbf{g}_{i,t}^{\mathbf{x}} + \frac{\epsilon_{u_{i,t}}^{\mathbf{x}}}{|\mathcal{A}_{i,t}^{\mathbf{x}}|} + \frac{\epsilon_{d_{y,i,t}}^{\mathbf{x}}}{|\mathcal{A}_{i,t}^{\mathbf{x}}|} \right) + \frac{1}{|\mathcal{A}_{\tau,t}|} \sum_{\mathbf{x} \in \mathcal{C}} \sum_{\mathbf{y} \in \mathcal{A}_{\tau,t}^{\mathbf{x}}} \left(\mathbf{w}_{\mathbf{y}_0,0,t}^o + \frac{\epsilon_{dy,t-1}}{|\mathcal{A}_{\tau,t-1}|} \right. \\
&\quad \left. - \frac{\epsilon_{dy_0,t-1}}{|\mathcal{A}_{\tau,t-1}|} \right) + \frac{\epsilon_{ut}}{|\mathcal{A}_{\tau,t}|} + \frac{\epsilon_{dy_0,t}}{|\mathcal{A}_{\tau,t}|} = -\frac{\mu_t}{|\mathcal{A}_{\tau,t}|} \sum_{\mathbf{x} \in \mathcal{C}} |\mathcal{A}_{\tau,t}^{\mathbf{x}}| \sum_{i=0}^{\tau-1} \mathbf{g}_{i,t}^{\mathbf{x}} - \frac{\mu_t}{|\mathcal{A}_{\tau,t}|} \sum_{\mathbf{x} \in \mathcal{C}} \sum_{\mathbf{y} \in \mathcal{A}_{\tau,t}^{\mathbf{x}}} \sum_{i=0}^{\tau-1} \\
&\quad \left(\frac{\epsilon_{u_{i,t}}^{\mathbf{x}}}{|\mathcal{A}_{i,t}^{\mathbf{x}}|} + \frac{\epsilon_{d_{y,i,t}}^{\mathbf{x}}}{|\mathcal{A}_{i,t}^{\mathbf{x}}|} \right) + \frac{1}{|\mathcal{A}_{\tau,t}|} \sum_{\mathbf{x} \in \mathcal{C}} \sum_{\mathbf{y} \in \mathcal{A}_{\tau,t}^{\mathbf{x}}} \left(\frac{\epsilon_{dy,t-1}}{|\mathcal{A}_{\tau,t-1}|} - \frac{\epsilon_{dy_0,t-1}}{|\mathcal{A}_{\tau,t-1}|} \right) + \frac{\epsilon_{ut}}{|\mathcal{A}_{\tau,t}|} + \frac{\epsilon_{dy_0,t}}{|\mathcal{A}_{\tau,t}|} + \mathbf{w}_{y_0,0,t}^o \\
&= -\frac{\mu_t}{|\mathcal{A}_{\tau,t}|} \sum_{\mathbf{x} \in \mathcal{C}} |\mathcal{A}_{\tau,t}^{\mathbf{x}}| \sum_{i=0}^{\tau-1} \mathbf{g}_{i,t}^{\mathbf{x}} - \frac{\mu_t}{|\mathcal{A}_{\tau,t}|} \sum_{\mathbf{x} \in \mathcal{C}} |\mathcal{A}_{\tau,t}^{\mathbf{x}}| \sum_{i=0}^{\tau-1} \frac{\epsilon_{u_{i,t}}^{\mathbf{x}}}{|\mathcal{A}_{i,t}^{\mathbf{x}}|} - \frac{\mu_t}{|\mathcal{A}_{\tau,t}|} \sum_{\mathbf{x} \in \mathcal{C}} \sum_{\mathbf{y} \in \mathcal{A}_{\tau,t}^{\mathbf{x}}} \sum_{i=0}^{\tau-1} \frac{\epsilon_{d_{y,i,t}}^{\mathbf{x}}}{|\mathcal{A}_{i,t}^{\mathbf{x}}|} \\
&\quad + \frac{1}{|\mathcal{A}_{\tau,t}|} \sum_{\mathbf{x} \in \mathcal{C}} \sum_{\mathbf{y} \in \mathcal{A}_{\tau,t}^{\mathbf{x}}} \left(\frac{\epsilon_{dy,t-1}}{|\mathcal{A}_{\tau,t-1}|} - \frac{\epsilon_{dy_0,t-1}}{|\mathcal{A}_{\tau,t-1}|} \right) + \frac{\epsilon_{ut}}{|\mathcal{A}_{\tau,t}|} + \frac{\epsilon_{dy_0,t}}{|\mathcal{A}_{\tau,t}|} + \mathbf{w}_{y_0,0,t}^o. \tag{45}
\end{aligned}$$

According to (45) and the L -Lipschitz continuous property in Assumption 1, we have

$$F(\mathbf{w}_{y_0,0,t+1}^o) - F(\mathbf{w}_{y_0,0,t}^o) \leq \nabla F(\mathbf{w}_{y_0,0,t}^o)^\top (\mathbf{w}_{y_0,0,t+1}^o - \mathbf{w}_{y_0,0,t}^o) + \frac{L}{2} \|\mathbf{w}_{y_0,0,t+1}^o - \mathbf{w}_{y_0,0,t}^o\|^2$$

$$\begin{aligned}
&= \nabla F(\mathbf{w}_{y_0,0,t}^o)^\top \left(-\frac{\mu_t}{|\mathcal{A}_{\tau,t}|} \sum_{\mathbf{x} \in \mathcal{C}} |\mathcal{A}_{\tau,t}^{\mathbf{x}}| \sum_{i=0}^{\tau-1} \mathbf{g}_{i,t}^{\mathbf{x}} - \frac{\mu_t}{|\mathcal{A}_{\tau,t}|} \sum_{\mathbf{x} \in \mathcal{C}} |\mathcal{A}_{\tau,t}^{\mathbf{x}}| \sum_{i=0}^{\tau-1} \frac{\boldsymbol{\epsilon}_{u_{i,t}}^{\mathbf{x}}}{|\mathcal{A}_{i,t}^{\mathbf{x}}|} \right. \\
&\quad \left. - \frac{\mu_t}{|\mathcal{A}_{\tau,t}|} \sum_{\mathbf{x} \in \mathcal{C}} \sum_{\mathbf{y} \in \mathcal{A}_{\tau,t}^{\mathbf{x}}} \sum_{i=0}^{\tau-1} \frac{\boldsymbol{\epsilon}_{d_{y,i,t}}^{\mathbf{x}}}{|\mathcal{A}_{i,t}^{\mathbf{x}}|} + \frac{1}{|\mathcal{A}_{\tau,t}|} \sum_{\mathbf{x} \in \mathcal{C}} \sum_{\mathbf{y} \in \mathcal{A}_{\tau,t}^{\mathbf{x}}} \left(\frac{\boldsymbol{\epsilon}_{d_{y,t-1}}}{|\mathcal{A}_{\tau,t-1}|} - \frac{\boldsymbol{\epsilon}_{d_{y_0,t-1}}}{|\mathcal{A}_{\tau,t-1}|} \right) + \frac{\boldsymbol{\epsilon}_{u_t}}{|\mathcal{A}_{\tau,t}|} + \frac{\boldsymbol{\epsilon}_{d_{y_0,t}}}{|\mathcal{A}_{\tau,t}|} \right) \\
&\quad + \frac{L}{2} \left\| -\frac{\mu_t}{|\mathcal{A}_{\tau,t}|} \sum_{\mathbf{x} \in \mathcal{C}} |\mathcal{A}_{\tau,t}^{\mathbf{x}}| \sum_{i=0}^{\tau-1} \mathbf{g}_{i,t}^{\mathbf{x}} - \frac{\mu_t}{|\mathcal{A}_{\tau,t}|} \sum_{\mathbf{x} \in \mathcal{C}} |\mathcal{A}_{\tau,t}^{\mathbf{x}}| \sum_{i=0}^{\tau-1} \frac{\boldsymbol{\epsilon}_{u_{i,t}}^{\mathbf{x}}}{|\mathcal{A}_{i,t}^{\mathbf{x}}|} \right. \\
&\quad \left. - \frac{\mu_t}{|\mathcal{A}_{\tau,t}|} \sum_{\mathbf{x} \in \mathcal{C}} \sum_{\mathbf{y} \in \mathcal{A}_{\tau,t}^{\mathbf{x}}} \sum_{i=0}^{\tau-1} \frac{\boldsymbol{\epsilon}_{d_{y,i,t}}^{\mathbf{x}}}{|\mathcal{A}_{i,t}^{\mathbf{x}}|} + \frac{1}{|\mathcal{A}_{\tau,t}|} \sum_{\mathbf{x} \in \mathcal{C}} \sum_{\mathbf{y} \in \mathcal{A}_{\tau,t}^{\mathbf{x}}} \left(\frac{\boldsymbol{\epsilon}_{d_{y,t-1}}}{|\mathcal{A}_{\tau,t-1}|} - \frac{\boldsymbol{\epsilon}_{d_{y_0,t-1}}}{|\mathcal{A}_{\tau,t-1}|} \right) + \frac{\boldsymbol{\epsilon}_{u_t}}{|\mathcal{A}_{\tau,t}|} + \frac{\boldsymbol{\epsilon}_{d_{y_0,t}}}{|\mathcal{A}_{\tau,t}|} \right\|^2.
\end{aligned} \tag{46}$$

By taking expectation on both sides of (46) and considering the independency of error terms, we continue as

$$\begin{aligned}
\mathbb{E} \{ F(\mathbf{w}_{y_0,0,t+1}^o) - F(\mathbf{w}_{y_0,0,t}^o) \} &\leq -\frac{\mu_t}{|\mathcal{A}_{\tau,t}|} \sum_{\mathbf{x} \in \mathcal{C}} |\mathcal{A}_{\tau,t}^{\mathbf{x}}| \sum_{i=0}^{\tau-1} \mathbb{E} \{ \nabla F(\mathbf{w}_{y_0,0,t}^o)^\top \mathbf{g}_{i,t}^{\mathbf{x}} \} \\
&\quad + \frac{L\mu_t^2}{2} \mathbb{E} \left\{ \left\| \sum_{\mathbf{x} \in \mathcal{C}} \frac{|\mathcal{A}_{\tau,t}^{\mathbf{x}}|}{|\mathcal{A}_{\tau,t}|} \sum_{i=0}^{\tau-1} \mathbf{g}_{i,t}^{\mathbf{x}} \right\|^2 \right\} + \frac{L\mu_t^2}{2|\mathcal{A}_{\tau,t}|^2} \sum_{\mathbf{x} \in \mathcal{C}} |\mathcal{A}_{\tau,t}^{\mathbf{x}}|^2 \sum_{i=0}^{\tau-1} \frac{\mathbb{E} \{ \|\boldsymbol{\epsilon}_{u_{i,t}}^{\mathbf{x}}\|^2 \}}{|\mathcal{A}_{i,t}^{\mathbf{x}}|^2} \\
&\quad + \frac{L\mu_t^2}{2|\mathcal{A}_{\tau,t}|^2} \sum_{\mathbf{x} \in \mathcal{C}} \sum_{\mathbf{y} \in \mathcal{A}_{\tau,t}^{\mathbf{x}}} \sum_{i=0}^{\tau-1} \frac{\mathbb{E} \{ \|\boldsymbol{\epsilon}_{d_{y,i,t}}^{\mathbf{x}}\|^2 \}}{|\mathcal{A}_{i,t}^{\mathbf{x}}|^2} + \frac{L}{2|\mathcal{A}_{\tau,t}|^2} \sum_{\mathbf{x} \in \mathcal{C}} \sum_{\mathbf{y} \in \mathcal{A}_{\tau,t}^{\mathbf{x}}} \frac{\mathbb{E} \{ \|\boldsymbol{\epsilon}_{d_{y,t-1}}\|^2 \}}{|\mathcal{A}_{\tau,t-1}|^2} \\
&\quad + \frac{L}{2} \frac{\mathbb{E} \{ \|\boldsymbol{\epsilon}_{d_{y_0,t-1}}\|^2 \}}{|\mathcal{A}_{\tau,t-1}|^2} + \frac{L}{2} \frac{\mathbb{E} \{ \|\boldsymbol{\epsilon}_{u_t}\|^2 \}}{|\mathcal{A}_{\tau,t}|^2} + \frac{L}{2} \frac{\mathbb{E} \{ \|\boldsymbol{\epsilon}_{d_{y_0,t}}\|^2 \}}{|\mathcal{A}_{\tau,t}|^2}.
\end{aligned} \tag{47}$$

Next, we bound the first term of the right-hand side (RHS) in (47). We can write its inner-sum term as

$$\begin{aligned}
\mathbb{E} \{ \nabla F(\mathbf{w}_{y_0,0,t}^o)^\top \mathbf{g}_{i,t}^{\mathbf{x}} \} &= \mathbb{E} \left\{ \nabla F(\mathbf{w}_{y_0,0,t}^o)^\top \frac{1}{|\mathcal{A}_{i,t}^{\mathbf{x}}|} \sum_{\mathbf{y} \in \mathcal{A}_{i,t}^{\mathbf{x}}} \nabla F_{\mathbf{y}}^{\mathbf{x}}(\mathbf{w}_{\mathbf{y},i,t}^{\mathbf{x}}) \right\} \\
&= \mathbb{E} \left\{ \frac{1}{|\mathcal{A}_{i,t}^{\mathbf{x}}|} \sum_{\mathbf{y} \in \mathcal{A}_{i,t}^{\mathbf{x}}} \nabla F(\mathbf{w}_{y_0,0,t}^o)^\top \nabla F_{\mathbf{y}}^{\mathbf{x}}(\mathbf{w}_{\mathbf{y},i,t}^{\mathbf{x}}) \right\} = \frac{1}{|\mathcal{A}_{i,t}^{\mathbf{x}}|} \sum_{\mathbf{y} \in \mathcal{A}_{i,t}^{\mathbf{x}}} \mathbb{E} \{ \nabla F(\mathbf{w}_{y_0,0,t}^o)^\top \nabla F(\mathbf{w}_{\mathbf{y},i,t}^{\mathbf{x}}) \}.
\end{aligned} \tag{48}$$

Using the equality $\|\mathbf{a}_1 - \mathbf{a}_2\|^2 = \|\mathbf{a}_1\|^2 + \|\mathbf{a}_2\|^2 - 2\mathbf{a}_1^\top \mathbf{a}_2$ for any vectors \mathbf{a}_1 and \mathbf{a}_2 , the term in the sum in (48) can be written as

$$\begin{aligned}
\mathbb{E} \{ \nabla F(\mathbf{w}_{y_0,0,t}^o)^\top \nabla F(\mathbf{w}_{\mathbf{y},i,t}^{\mathbf{x}}) \} &= \frac{1}{2} \mathbb{E} \{ \|\nabla F(\mathbf{w}_{y_0,0,t}^o)\|^2 \} + \frac{1}{2} \mathbb{E} \{ \|\nabla F(\mathbf{w}_{\mathbf{y},i,t}^{\mathbf{x}})\|^2 \} \\
&\quad - \frac{1}{2} \mathbb{E} \{ \|\nabla F(\mathbf{w}_{y_0,0,t}^o) - \nabla F(\mathbf{w}_{\mathbf{y},i,t}^{\mathbf{x}})\|^2 \}.
\end{aligned} \tag{49}$$

From Assumption 1, the last term in (49) is bounded as

$$\begin{aligned}
& \mathbb{E} \left\{ \|\nabla F(\mathbf{w}_{\mathbf{y}_0,0,t}^{\circ}) - \nabla F(\mathbf{w}_{\mathbf{y},i,t}^{\mathbf{x}})\|^2 \right\} \leq L^2 \mathbb{E} \left\{ \|\mathbf{w}_{\mathbf{y}_0,0,t}^{\circ} - \mathbf{w}_{\mathbf{y},i,t}^{\mathbf{x}}\|^2 \right\} = L^2 \times \\
& \mathbb{E} \left\{ \left\| \mathbf{w}_{\mathbf{y},0,t}^{\mathbf{x}} - \frac{\boldsymbol{\epsilon}_{\mathbf{d}\mathbf{y},t-1}}{|\mathcal{A}_{\tau,t-1}|} + \frac{\boldsymbol{\epsilon}_{\mathbf{d}\mathbf{y}_0,t-1}}{|\mathcal{A}_{\tau,t-1}|} - \mathbf{w}_{\mathbf{y},i,t}^{\mathbf{x}} \right\|^2 \right\} = L^2 \mathbb{E} \left\{ \left\| -\mu_t \sum_{j=0}^{i-1} \mathbf{g}_{\mathbf{y},j,t}^{\mathbf{x}} - \frac{\boldsymbol{\epsilon}_{\mathbf{d}\mathbf{y},t-1}}{|\mathcal{A}_{\tau,t-1}|} + \frac{\boldsymbol{\epsilon}_{\mathbf{d}\mathbf{y}_0,t-1}}{|\mathcal{A}_{\tau,t-1}|} \right\|^2 \right\} \\
& = L^2 \mu_t^2 \mathbb{E} \left\{ \left\| \sum_{j=0}^{i-1} \mathbf{g}_{\mathbf{y},j,t}^{\mathbf{x}} \right\|^2 \right\} + L^2 \frac{\mathbb{E} \left\{ \|\boldsymbol{\epsilon}_{\mathbf{d}\mathbf{y},t-1}\|^2 \right\}}{|\mathcal{A}_{\tau,t-1}|^2} + L^2 \frac{\mathbb{E} \left\{ \|\boldsymbol{\epsilon}_{\mathbf{d}\mathbf{y}_0,t-1}\|^2 \right\}}{|\mathcal{A}_{\tau,t-1}|^2} \\
& = L^2 \mu_t^2 \mathbb{E} \left\{ \left\| \sum_{j=0}^{i-1} \mathbf{g}_{j,t}^{\mathbf{x}} + \frac{\boldsymbol{\epsilon}_{\mathbf{u}_{j,t}^{\mathbf{x}}}}{|\mathcal{A}_{j,t}^{\mathbf{x}}|} + \frac{\boldsymbol{\epsilon}_{\mathbf{d}\mathbf{y},j,t}^{\mathbf{x}}}{|\mathcal{A}_{j,t}^{\mathbf{x}}|} \right\|^2 \right\} + L^2 \frac{\mathbb{E} \left\{ \|\boldsymbol{\epsilon}_{\mathbf{d}\mathbf{y},t-1}\|^2 \right\}}{|\mathcal{A}_{\tau,t-1}|^2} + L^2 \frac{\mathbb{E} \left\{ \|\boldsymbol{\epsilon}_{\mathbf{d}\mathbf{y}_0,t-1}\|^2 \right\}}{|\mathcal{A}_{\tau,t-1}|^2} \\
& = L^2 \mu_t^2 \mathbb{E} \left\{ \left\| \sum_{j=0}^{i-1} \mathbf{g}_{j,t}^{\mathbf{x}} \right\|^2 \right\} + L^2 \mu_t^2 \sum_{j=0}^{i-1} \frac{\mathbb{E} \left\{ \|\boldsymbol{\epsilon}_{\mathbf{u}_{j,t}^{\mathbf{x}}}\|^2 \right\}}{|\mathcal{A}_{j,t}^{\mathbf{x}}|^2} + L^2 \mu_t^2 \sum_{j=0}^{i-1} \frac{\mathbb{E} \left\{ \|\boldsymbol{\epsilon}_{\mathbf{d}\mathbf{y},j,t}^{\mathbf{x}}\|^2 \right\}}{|\mathcal{A}_{j,t}^{\mathbf{x}}|^2} \\
& + L^2 \frac{\mathbb{E} \left\{ \|\boldsymbol{\epsilon}_{\mathbf{d}\mathbf{y},t-1}\|^2 \right\}}{|\mathcal{A}_{\tau,t-1}|^2} + L^2 \frac{\mathbb{E} \left\{ \|\boldsymbol{\epsilon}_{\mathbf{d}\mathbf{y}_0,t-1}\|^2 \right\}}{|\mathcal{A}_{\tau,t-1}|^2}, \tag{50}
\end{aligned}$$

where using the equality $\mathbb{E} \left\{ \|\mathbf{a}\|^2 \right\} = \|\mathbb{E} \left\{ \mathbf{a} \right\}\|^2 + \mathbb{E} \left\{ \|\mathbf{a} - \mathbb{E} \left\{ \mathbf{a} \right\}\|^2 \right\}$ for a random vector \mathbf{a} , we have

$$\begin{aligned}
& \mathbb{E} \left\{ \left\| \sum_{j=0}^{i-1} \mathbf{g}_{j,t}^{\mathbf{x}} \right\|^2 \right\} = \\
& \mathbb{E} \left\{ \left\| \sum_{j=0}^{i-1} \frac{1}{|\mathcal{A}_{j,t}^{\mathbf{x}}|} \sum_{\mathbf{y} \in \mathcal{A}_{j,t}^{\mathbf{x}}} \nabla F_{\mathbf{y}}^{\mathbf{x}}(\mathbf{w}_{\mathbf{y},j,t}^{\mathbf{x}}) \right\|^2 \right\} = \mathbb{E} \left\{ \left\| \sum_{j=0}^{i-1} \frac{1}{|\mathcal{A}_{j,t}^{\mathbf{x}}|} \sum_{\mathbf{y} \in \mathcal{A}_{j,t}^{\mathbf{x}}} \nabla F(\mathbf{w}_{\mathbf{y},j,t}^{\mathbf{x}}) \right\|^2 \right\} \\
& + \mathbb{E} \left\{ \left\| \sum_{j=0}^{i-1} \frac{1}{|\mathcal{A}_{j,t}^{\mathbf{x}}|} \sum_{\mathbf{y} \in \mathcal{A}_{j,t}^{\mathbf{x}}} (\nabla F_{\mathbf{y}}^{\mathbf{x}}(\mathbf{w}_{\mathbf{y},j,t}^{\mathbf{x}}) - \nabla F(\mathbf{w}_{\mathbf{y},j,t}^{\mathbf{x}})) \right\|^2 \right\}, \tag{51}
\end{aligned}$$

where the first term of RHS can be upper-bounded as

$$\begin{aligned}
& \mathbb{E} \left\{ \left\| \sum_{j=0}^{i-1} \frac{1}{|\mathcal{A}_{j,t}^{\mathbf{x}}|} \sum_{\mathbf{y} \in \mathcal{A}_{j,t}^{\mathbf{x}}} \nabla F(\mathbf{w}_{\mathbf{y},j,t}^{\mathbf{x}}) \right\|^2 \right\} \stackrel{(a)}{\leq} i \sum_{j=0}^{i-1} \mathbb{E} \left\{ \left\| \frac{1}{|\mathcal{A}_{j,t}^{\mathbf{x}}|} \sum_{\mathbf{y} \in \mathcal{A}_{j,t}^{\mathbf{x}}} \nabla F(\mathbf{w}_{\mathbf{y},j,t}^{\mathbf{x}}) \right\|^2 \right\} \\
& \stackrel{(b)}{\leq} i \sum_{j=0}^{i-1} \frac{1}{|\mathcal{A}_{j,t}^{\mathbf{x}}|} \sum_{\mathbf{y} \in \mathcal{A}_{j,t}^{\mathbf{x}}} \mathbb{E} \left\{ \|\nabla F(\mathbf{w}_{\mathbf{y},j,t}^{\mathbf{x}})\|^2 \right\}, \tag{52}
\end{aligned}$$

where (a) comes from the inequality of arithmetic and geometric means, i.e., $(\sum_{i=1}^I a_i)^2 \leq I \sum_{i=1}^I a_i^2$, and (b) is from the convexity of the function $\|\cdot\|^2$. The second term of RHS in (51)

can be upper-bounded as

$$\begin{aligned}
& \mathbb{E} \left\{ \left\| \sum_{j=0}^{i-1} \frac{1}{|\mathcal{A}_{j,t}^x|} \sum_{\mathbf{y} \in \mathcal{A}_{j,t}^x} (\nabla F_{\mathbf{y}}^x(\mathbf{w}_{\mathbf{y},j,t}^x) - \nabla F(\mathbf{w}_{\mathbf{y},j,t}^x)) \right\|^2 \right\} \\
& \stackrel{(c)}{=} \sum_{j=0}^{i-1} \mathbb{E} \left\{ \left\| \frac{1}{|\mathcal{A}_{j,t}^x|} \sum_{\mathbf{y} \in \mathcal{A}_{j,t}^x} (\nabla F_{\mathbf{y}}^x(\mathbf{w}_{\mathbf{y},j,t}^x) - \nabla F(\mathbf{w}_{\mathbf{y},j,t}^x)) \right\|^2 \right\} \\
& \stackrel{(d)}{=} \sum_{j=0}^{i-1} \frac{1}{|\mathcal{A}_{j,t}^x|^2} \sum_{\mathbf{y} \in \mathcal{A}_{j,t}^x} \mathbb{E} \left\{ \|\nabla F_{\mathbf{y}}^x(\mathbf{w}_{\mathbf{y},j,t}^x) - \nabla F(\mathbf{w}_{\mathbf{y},j,t}^x)\|^2 \right\} \\
& \stackrel{(e)}{\leq} \sum_{j=0}^{i-1} \frac{1}{|\mathcal{A}_{j,t}^x|^2} \sum_{\mathbf{y} \in \mathcal{A}_{j,t}^x} \frac{\sigma^2}{B} = \frac{\sigma^2}{B} \sum_{j=0}^{i-1} \frac{1}{|\mathcal{A}_{j,t}^x|}, \tag{53}
\end{aligned}$$

where (c) and (d) are due to the fact that for any $\mathbf{y}_1 \neq \mathbf{y}_2, j_1 \neq j_2$

$$\begin{aligned}
& \mathbb{E} \left\{ (\nabla F_{\mathbf{y}_1}^x(\mathbf{w}_{\mathbf{y}_1,j_1,t}^x) - \nabla F(\mathbf{w}_{\mathbf{y}_1,j_1,t}^x))^\top (\nabla F_{\mathbf{y}_2}^x(\mathbf{w}_{\mathbf{y}_2,j_2,t}^x) - \nabla F(\mathbf{w}_{\mathbf{y}_2,j_2,t}^x)) \right\} \\
& = \mathbb{E} \left\{ \mathbb{E}_{\mathcal{D}_{\mathbf{y}_1,j_1}^x} \left\{ (\nabla F_{\mathbf{y}_1}^x(\mathbf{w}_{\mathbf{y}_1,j_1,t}^x) - \nabla F(\mathbf{w}_{\mathbf{y}_1,j_1,t}^x))^\top \right\} (\nabla F_{\mathbf{y}_2}^x(\mathbf{w}_{\mathbf{y}_2,j_2,t}^x) - \nabla F(\mathbf{w}_{\mathbf{y}_2,j_2,t}^x)) \mid \mathcal{D}_{\mathbf{y}_1,j_1}^x \right\} \\
& = 0, \tag{54}
\end{aligned}$$

where $\mathbb{E}_{\mathcal{D}_{\mathbf{y}_1,j_1}^x} \left\{ (\nabla F_{\mathbf{y}_1}^x(\mathbf{w}_{\mathbf{y}_1,j_1,t}^x) - \nabla F(\mathbf{w}_{\mathbf{y}_1,j_1,t}^x)) \right\} = \mathbf{0}$. Then, (e) comes from the Assumption

2. Replacing (52) and (53) in (51) and then replacing the result in (50), we have

$$\begin{aligned}
& \mathbb{E} \left\{ \|\nabla F(\mathbf{w}_{\mathbf{y}_0,0,t}^o) - \nabla F(\mathbf{w}_{\mathbf{y},i,t}^x)\|^2 \right\} \leq \\
& L^2 \mu_t^2 i \sum_{j=0}^{i-1} \frac{1}{|\mathcal{A}_{j,t}^x|} \sum_{\mathbf{y} \in \mathcal{A}_{j,t}^x} \mathbb{E} \left\{ \|\nabla F(\mathbf{w}_{\mathbf{y},j,t}^x)\|^2 \right\} + L^2 \mu_t^2 \frac{\sigma^2}{B} \sum_{j=0}^{i-1} \frac{1}{|\mathcal{A}_{j,t}^x|} + L^2 \mu_t^2 \sum_{j=0}^{i-1} \frac{\mathbb{E} \left\{ \|\epsilon_{\mathbf{u}_{j,t}^x}\|^2 \right\}}{|\mathcal{A}_{j,t}^x|^2} \\
& + L^2 \mu_t^2 \sum_{j=0}^{i-1} \frac{\mathbb{E} \left\{ \|\epsilon_{\mathbf{d}_{\mathbf{y},j,t}^x}\|^2 \right\}}{|\mathcal{A}_{j,t}^x|^2} + L^2 \frac{\mathbb{E} \left\{ \|\epsilon_{\mathbf{d}_{\mathbf{y},t-1}\}\|^2 \right\}}{|\mathcal{A}_{\tau,t-1}|^2} + L^2 \frac{\mathbb{E} \left\{ \|\epsilon_{\mathbf{d}_{\mathbf{y}_0,t-1}\}\|^2 \right\}}{|\mathcal{A}_{\tau,t-1}|^2}, \tag{55}
\end{aligned}$$

and then replacing (55) in (49) and replacing the result in (48), we obtain the following bound

$$\begin{aligned}
& - \frac{\mu_t}{|\mathcal{A}_{\tau,t}|} \sum_{\mathbf{x} \in \mathcal{C}} |\mathcal{A}_{\tau,t}^x| \sum_{i=0}^{\tau-1} \mathbb{E} \left\{ \nabla F(\mathbf{w}_{\mathbf{y}_0,0,t}^o)^\top \mathbf{g}_{i,t}^x \right\} \leq - \frac{\mu_t \tau}{2} \mathbb{E} \left\{ \|\nabla F(\mathbf{w}_{\mathbf{y}_0,0,t}^o)\|^2 \right\} \\
& - \frac{\mu_t}{2|\mathcal{A}_{\tau,t}|} \sum_{\mathbf{x} \in \mathcal{C}} |\mathcal{A}_{\tau,t}^x| \sum_{i=0}^{\tau-1} \frac{1}{|\mathcal{A}_{i,t}^x|} \sum_{\mathbf{y} \in \mathcal{A}_{i,t}^x} \mathbb{E} \left\{ \|\nabla F(\mathbf{w}_{\mathbf{y},i,t}^x)\|^2 \right\} \\
& + \frac{L^2 \mu_t^3}{2|\mathcal{A}_{\tau,t}|} \sum_{\mathbf{x} \in \mathcal{C}} |\mathcal{A}_{\tau,t}^x| \sum_{i=0}^{\tau-1} i \sum_{j=0}^{i-1} \frac{1}{|\mathcal{A}_{j,t}^x|} \sum_{\mathbf{y} \in \mathcal{A}_{j,t}^x} \mathbb{E} \left\{ \|\nabla F(\mathbf{w}_{\mathbf{y},j,t}^x)\|^2 \right\} \\
& + \frac{L^2 \mu_t^3}{2|\mathcal{A}_{\tau,t}|} \frac{\sigma^2}{B} \sum_{\mathbf{x} \in \mathcal{C}} |\mathcal{A}_{\tau,t}^x| \sum_{i=0}^{\tau-1} \sum_{j=0}^{i-1} \frac{1}{|\mathcal{A}_{j,t}^x|} + \frac{L^2 \mu_t^3}{2|\mathcal{A}_{\tau,t}|} \sum_{\mathbf{x} \in \mathcal{C}} |\mathcal{A}_{\tau,t}^x| \sum_{i=0}^{\tau-1} \sum_{j=0}^{i-1} \frac{\mathbb{E} \left\{ \|\epsilon_{\mathbf{u}_{j,t}^x}\|^2 \right\}}{|\mathcal{A}_{j,t}^x|^2}
\end{aligned}$$

$$\begin{aligned}
& + \frac{L^2 \mu_t^3}{2|\mathcal{A}_{\tau,t}|} \sum_{\mathbf{x} \in \mathcal{C}} |\mathcal{A}_{\tau,t}^{\mathbf{x}}| \sum_{i=0}^{\tau-1} \frac{1}{|\mathcal{A}_{i,t}^{\mathbf{x}}|} \sum_{\mathbf{y} \in \mathcal{A}_{i,t}^{\mathbf{x}}} \sum_{j=0}^{i-1} \frac{\mathbb{E} \{ \|\epsilon_{\mathbf{d}_{\mathbf{y},j,t}}^{\mathbf{x}}\|^2 \}}{|\mathcal{A}_{j,t}^{\mathbf{x}}|^2} \\
& + \frac{L^2 \mu_t}{2|\mathcal{A}_{\tau,t}|} \sum_{\mathbf{x} \in \mathcal{C}} |\mathcal{A}_{\tau,t}^{\mathbf{x}}| \sum_{i=0}^{\tau-1} \frac{1}{|\mathcal{A}_{i,t}^{\mathbf{x}}|} \sum_{\mathbf{y} \in \mathcal{A}_{i,t}^{\mathbf{x}}} \frac{\mathbb{E} \{ \|\epsilon_{\mathbf{d}_{\mathbf{y},t-1}}^{\mathbf{x}}\|^2 \}}{|\mathcal{A}_{\tau,t-1}|^2} + \frac{L^2 \mu_t \tau}{2} \frac{\mathbb{E} \{ \|\epsilon_{\mathbf{d}_{\mathbf{y}_0,t-1}}^{\mathbf{x}}\|^2 \}}{|\mathcal{A}_{\tau,t-1}|^2}. \tag{56}
\end{aligned}$$

Next, we bound the second term of the RHS in (47) as

$$\begin{aligned}
& \mathbb{E} \left\{ \left\| \sum_{\mathbf{x} \in \mathcal{C}} \frac{|\mathcal{A}_{\tau,t}^{\mathbf{x}}|}{|\mathcal{A}_{\tau,t}|} \sum_{i=0}^{\tau-1} \mathbf{g}_{i,t}^{\mathbf{x}} \right\|^2 \right\} = \mathbb{E} \left\{ \left\| \sum_{\mathbf{x} \in \mathcal{C}} \frac{|\mathcal{A}_{\tau,t}^{\mathbf{x}}|}{|\mathcal{A}_{\tau,t}|} \sum_{i=0}^{\tau-1} \frac{1}{|\mathcal{A}_{i,t}^{\mathbf{x}}|} \sum_{\mathbf{y} \in \mathcal{A}_{i,t}^{\mathbf{x}}} \nabla F_{\mathbf{y}}^{\mathbf{x}}(\mathbf{w}_{\mathbf{y},i,t}^{\mathbf{x}}) \right\|^2 \right\} \\
& = \mathbb{E} \left\{ \left\| \sum_{\mathbf{x} \in \mathcal{C}} \frac{|\mathcal{A}_{\tau,t}^{\mathbf{x}}|}{|\mathcal{A}_{\tau,t}|} \sum_{i=0}^{\tau-1} \frac{1}{|\mathcal{A}_{i,t}^{\mathbf{x}}|} \sum_{\mathbf{y} \in \mathcal{A}_{i,t}^{\mathbf{x}}} \nabla F(\mathbf{w}_{\mathbf{y},i,t}^{\mathbf{x}}) \right\|^2 \right\} \\
& + \mathbb{E} \left\{ \left\| \sum_{\mathbf{x} \in \mathcal{C}} \frac{|\mathcal{A}_{\tau,t}^{\mathbf{x}}|}{|\mathcal{A}_{\tau,t}|} \sum_{i=0}^{\tau-1} \frac{1}{|\mathcal{A}_{i,t}^{\mathbf{x}}|} \sum_{\mathbf{y} \in \mathcal{A}_{i,t}^{\mathbf{x}}} (\nabla F_{\mathbf{y}}^{\mathbf{x}}(\mathbf{w}_{\mathbf{y},i,t}^{\mathbf{x}}) - \nabla F(\mathbf{w}_{\mathbf{y},i,t}^{\mathbf{x}})) \right\|^2 \right\}, \tag{57}
\end{aligned}$$

where

$$\begin{aligned}
& \mathbb{E} \left\{ \left\| \sum_{\mathbf{x} \in \mathcal{C}} \frac{|\mathcal{A}_{\tau,t}^{\mathbf{x}}|}{|\mathcal{A}_{\tau,t}|} \sum_{i=0}^{\tau-1} \frac{1}{|\mathcal{A}_{i,t}^{\mathbf{x}}|} \sum_{\mathbf{y} \in \mathcal{A}_{i,t}^{\mathbf{x}}} \nabla F(\mathbf{w}_{\mathbf{y},i,t}^{\mathbf{x}}) \right\|^2 \right\} \\
& \stackrel{(f)}{\leq} \sum_{\mathbf{x} \in \mathcal{C}} \frac{|\mathcal{A}_{\tau,t}^{\mathbf{x}}|}{|\mathcal{A}_{\tau,t}|} \mathbb{E} \left\{ \left\| \sum_{i=0}^{\tau-1} \frac{1}{|\mathcal{A}_{i,t}^{\mathbf{x}}|} \sum_{\mathbf{y} \in \mathcal{A}_{i,t}^{\mathbf{x}}} \nabla F(\mathbf{w}_{\mathbf{y},i,t}^{\mathbf{x}}) \right\|^2 \right\} \\
& \stackrel{(g)}{\leq} \tau \sum_{\mathbf{x} \in \mathcal{C}} \frac{|\mathcal{A}_{\tau,t}^{\mathbf{x}}|}{|\mathcal{A}_{\tau,t}|} \sum_{i=0}^{\tau-1} \mathbb{E} \left\{ \left\| \frac{1}{|\mathcal{A}_{i,t}^{\mathbf{x}}|} \sum_{\mathbf{y} \in \mathcal{A}_{i,t}^{\mathbf{x}}} \nabla F(\mathbf{w}_{\mathbf{y},i,t}^{\mathbf{x}}) \right\|^2 \right\} \\
& \stackrel{(h)}{\leq} \tau \sum_{\mathbf{x} \in \mathcal{C}} \frac{|\mathcal{A}_{\tau,t}^{\mathbf{x}}|}{|\mathcal{A}_{\tau,t}|} \sum_{i=0}^{\tau-1} \frac{1}{|\mathcal{A}_{i,t}^{\mathbf{x}}|} \sum_{\mathbf{y} \in \mathcal{A}_{i,t}^{\mathbf{x}}} \mathbb{E} \left\{ \|\nabla F(\mathbf{w}_{\mathbf{y},i,t}^{\mathbf{x}})\|^2 \right\}, \tag{58}
\end{aligned}$$

where (f) and (h) follows from the convexity of $\|\cdot\|^2$, and (g) is from the inequality of arithmetic and geometric means. Also, the second term of RHS in (57) can be upper-bounded as

$$\begin{aligned}
& \mathbb{E} \left\{ \left\| \sum_{\mathbf{x} \in \mathcal{C}} \frac{|\mathcal{A}_{\tau,t}^{\mathbf{x}}|}{|\mathcal{A}_{\tau,t}|} \sum_{i=0}^{\tau-1} \frac{1}{|\mathcal{A}_{i,t}^{\mathbf{x}}|} \sum_{\mathbf{y} \in \mathcal{A}_{i,t}^{\mathbf{x}}} (\nabla F_{\mathbf{y}}^{\mathbf{x}}(\mathbf{w}_{\mathbf{y},i,t}^{\mathbf{x}}) - \nabla F(\mathbf{w}_{\mathbf{y},i,t}^{\mathbf{x}})) \right\|^2 \right\} \\
& \stackrel{(i)}{=} \sum_{\mathbf{x} \in \mathcal{C}} \frac{|\mathcal{A}_{\tau,t}^{\mathbf{x}}|^2}{|\mathcal{A}_{\tau,t}|^2} \sum_{i=0}^{\tau-1} \frac{1}{|\mathcal{A}_{i,t}^{\mathbf{x}}|^2} \sum_{\mathbf{y} \in \mathcal{A}_{i,t}^{\mathbf{x}}} \mathbb{E} \left\{ \|\nabla F_{\mathbf{y}}^{\mathbf{x}}(\mathbf{w}_{\mathbf{y},i,t}^{\mathbf{x}}) - \nabla F(\mathbf{w}_{\mathbf{y},i,t}^{\mathbf{x}})\|^2 \right\} \\
& \stackrel{(j)}{\leq} \sum_{\mathbf{x} \in \mathcal{C}} \frac{|\mathcal{A}_{\tau,t}^{\mathbf{x}}|^2}{|\mathcal{A}_{\tau,t}|^2} \sum_{i=0}^{\tau-1} \frac{1}{|\mathcal{A}_{i,t}^{\mathbf{x}}|^2} \sum_{\mathbf{y} \in \mathcal{A}_{i,t}^{\mathbf{x}}} \frac{\sigma^2}{B} = \frac{\sigma^2}{B} \sum_{\mathbf{x} \in \mathcal{C}} \frac{|\mathcal{A}_{\tau,t}^{\mathbf{x}}|^2}{|\mathcal{A}_{\tau,t}|^2} \sum_{i=0}^{\tau-1} \frac{1}{|\mathcal{A}_{i,t}^{\mathbf{x}}|}, \tag{59}
\end{aligned}$$

where (i) is due to the independency and (j) is from the Assumption 2. Now, replacing (58) and (59) in (57) and replacing the result with (56) in (47) and then using the bound

$$\sum_{i=0}^{\tau-1} i \sum_{j=0}^{i-1} \frac{1}{|\mathcal{A}_{j,t}^x|} \sum_{\mathbf{y} \in \mathcal{A}_{j,t}^x} \mathbb{E} \{ \|\nabla F(\mathbf{w}_{\mathbf{y},j,t}^x)\|^2 \} \leq \sum_{i=0}^{\tau-1} i \times \sum_{i=0}^{\tau-1} \frac{1}{|\mathcal{A}_{i,t}^x|} \sum_{\mathbf{y} \in \mathcal{A}_{i,t}^x} \mathbb{E} \{ \|\nabla F(\mathbf{w}_{\mathbf{y},i,t}^x)\|^2 \}$$

$$= \frac{\tau(\tau-1)}{2} \sum_{i=0}^{\tau-1} \frac{1}{|\mathcal{A}_{i,t}^x|} \sum_{\mathbf{y} \in \mathcal{A}_{i,t}^x} \mathbb{E} \{ \|\nabla F(\mathbf{w}_{\mathbf{y},i,t}^x)\|^2 \}, \text{ we obtain}$$

$$\begin{aligned} & \mathbb{E} \{ F(\mathbf{w}_{\mathbf{y}_0,0,t+1}^o) - F(\mathbf{w}_{\mathbf{y}_0,0,t}^o) \} \leq -\frac{\mu_t \tau}{2} \mathbb{E} \{ \|\nabla F(\mathbf{w}_{\mathbf{y}_0,0,t}^o)\|^2 \} \\ & - \frac{\mu_t}{2|\mathcal{A}_{\tau,t}|} \sum_{\mathbf{x} \in \mathcal{C}} |\mathcal{A}_{\tau,t}^x| \sum_{i=0}^{\tau-1} \frac{1}{|\mathcal{A}_{i,t}^x|} \sum_{\mathbf{y} \in \mathcal{A}_{i,t}^x} \mathbb{E} \{ \|\nabla F(\mathbf{w}_{\mathbf{y},i,t}^x)\|^2 \} \\ & + \frac{L^2 \mu_t^3}{2|\mathcal{A}_{\tau,t}|} \frac{\tau(\tau-1)}{2} \sum_{\mathbf{x} \in \mathcal{C}} |\mathcal{A}_{\tau,t}^x| \sum_{i=0}^{\tau-1} \frac{1}{|\mathcal{A}_{i,t}^x|} \sum_{\mathbf{y} \in \mathcal{A}_{i,t}^x} \mathbb{E} \{ \|\nabla F(\mathbf{w}_{\mathbf{y},i,t}^x)\|^2 \} \\ & + \frac{L^2 \mu_t^3}{2|\mathcal{A}_{\tau,t}|} \frac{\sigma^2}{B} \sum_{\mathbf{x} \in \mathcal{C}} |\mathcal{A}_{\tau,t}^x| \sum_{i=0}^{\tau-1} \sum_{j=0}^{i-1} \frac{1}{|\mathcal{A}_{j,t}^x|} + \frac{L^2 \mu_t^3}{2|\mathcal{A}_{\tau,t}|} \sum_{\mathbf{x} \in \mathcal{C}} |\mathcal{A}_{\tau,t}^x| \sum_{i=0}^{\tau-1} \sum_{j=0}^{i-1} \frac{\mathbb{E} \{ \|\epsilon_{\mathbf{u}_{j,t}^x}\|^2 \}}{|\mathcal{A}_{j,t}^x|^2} \\ & + \frac{L^2 \mu_t^3}{2|\mathcal{A}_{\tau,t}|} \sum_{\mathbf{x} \in \mathcal{C}} |\mathcal{A}_{\tau,t}^x| \sum_{i=0}^{\tau-1} \frac{1}{|\mathcal{A}_{i,t}^x|} \sum_{\mathbf{y} \in \mathcal{A}_{i,t}^x} \sum_{j=0}^{i-1} \frac{\mathbb{E} \{ \|\epsilon_{\mathbf{d}_{\mathbf{y},j,t}^x}\|^2 \}}{|\mathcal{A}_{j,t}^x|^2} \\ & + \frac{L^2 \mu_t}{2|\mathcal{A}_{\tau,t}| |\mathcal{A}_{\tau,t-1}|^2} \sum_{\mathbf{x} \in \mathcal{C}} |\mathcal{A}_{\tau,t}^x| \sum_{i=0}^{\tau-1} \frac{1}{|\mathcal{A}_{i,t}^x|} \sum_{\mathbf{y} \in \mathcal{A}_{i,t}^x} \mathbb{E} \{ \|\epsilon_{\mathbf{d}_{\mathbf{y},t-1}\}\|^2 \} + \frac{L^2 \mu_t \tau}{2} \frac{\mathbb{E} \{ \|\epsilon_{\mathbf{d}_{\mathbf{y}_0,t-1}\}\|^2 \}}{|\mathcal{A}_{\tau,t-1}|^2} \\ & + \frac{L \mu_t^2 \tau}{2} \sum_{\mathbf{x} \in \mathcal{C}} \frac{|\mathcal{A}_{\tau,t}^x|}{|\mathcal{A}_{\tau,t}|} \sum_{i=0}^{\tau-1} \frac{1}{|\mathcal{A}_{i,t}^x|} \sum_{\mathbf{y} \in \mathcal{A}_{i,t}^x} \mathbb{E} \{ \|\nabla F(\mathbf{w}_{\mathbf{y},i,t}^x)\|^2 \} + \frac{L \mu_t^2 \sigma^2}{2} \frac{\sum_{\mathbf{x} \in \mathcal{C}} |\mathcal{A}_{\tau,t}^x|^2}{|\mathcal{A}_{\tau,t}|^2} \sum_{i=0}^{\tau-1} \frac{1}{|\mathcal{A}_{i,t}^x|} \\ & + \frac{L \mu_t^2}{2|\mathcal{A}_{\tau,t}|^2} \sum_{\mathbf{x} \in \mathcal{C}} |\mathcal{A}_{\tau,t}^x|^2 \sum_{i=0}^{\tau-1} \frac{\mathbb{E} \{ \|\epsilon_{\mathbf{u}_{i,t}^x}\|^2 \}}{|\mathcal{A}_{i,t}^x|^2} + \frac{L \mu_t^2}{2|\mathcal{A}_{\tau,t}|^2} \sum_{\mathbf{x} \in \mathcal{C}} \sum_{\mathbf{y} \in \mathcal{A}_{\tau,t}^x} \sum_{i=0}^{\tau-1} \frac{\mathbb{E} \{ \|\epsilon_{\mathbf{d}_{\mathbf{y},i,t}^x}\|^2 \}}{|\mathcal{A}_{i,t}^x|^2} \\ & + \frac{L}{2|\mathcal{A}_{\tau,t}|^2 |\mathcal{A}_{\tau,t-1}|^2} \sum_{\mathbf{x} \in \mathcal{C}} \sum_{\mathbf{y} \in \mathcal{A}_{\tau,t}^x} \mathbb{E} \{ \|\epsilon_{\mathbf{d}_{\mathbf{y},t-1}\}\|^2 \} + \frac{L}{2} \frac{\mathbb{E} \{ \|\epsilon_{\mathbf{d}_{\mathbf{y}_0,t-1}\}\|^2 \}}{|\mathcal{A}_{\tau,t-1}|^2} \\ & + \frac{L}{2} \frac{\mathbb{E} \{ \|\epsilon_{\mathbf{u}_t}\|^2 \}}{|\mathcal{A}_{\tau,t}|^2} + \frac{L}{2} \frac{\mathbb{E} \{ \|\epsilon_{\mathbf{d}_{\mathbf{y}_0,t}\}\|^2 \}}{|\mathcal{A}_{\tau,t}|^2}, \end{aligned} \tag{60}$$

where

$$\begin{aligned} & - \frac{\mu_t}{2|\mathcal{A}_{\tau,t}|} \sum_{\mathbf{x} \in \mathcal{C}} |\mathcal{A}_{\tau,t}^x| \sum_{i=0}^{\tau-1} \frac{1}{|\mathcal{A}_{i,t}^x|} \sum_{\mathbf{y} \in \mathcal{A}_{i,t}^x} \mathbb{E} \{ \|\nabla F(\mathbf{w}_{\mathbf{y},i,t}^x)\|^2 \} \\ & + \frac{L^2 \mu_t^3}{2|\mathcal{A}_{\tau,t}|} \frac{\tau(\tau-1)}{2} \sum_{\mathbf{x} \in \mathcal{C}} |\mathcal{A}_{\tau,t}^x| \sum_{i=0}^{\tau-1} \frac{1}{|\mathcal{A}_{i,t}^x|} \sum_{\mathbf{y} \in \mathcal{A}_{i,t}^x} \mathbb{E} \{ \|\nabla F(\mathbf{w}_{\mathbf{y},i,t}^x)\|^2 \} \\ & + \frac{L \mu_t^2 \tau}{2} \sum_{\mathbf{x} \in \mathcal{C}} \frac{|\mathcal{A}_{\tau,t}^x|}{|\mathcal{A}_{\tau,t}|} \sum_{i=0}^{\tau-1} \frac{1}{|\mathcal{A}_{i,t}^x|} \sum_{\mathbf{y} \in \mathcal{A}_{i,t}^x} \mathbb{E} \{ \|\nabla F(\mathbf{w}_{\mathbf{y},i,t}^x)\|^2 \} = \end{aligned}$$

$$-\frac{\mu_t}{2} \left(1 - \frac{L^2 \mu_t^2 \tau (\tau - 1)}{2} - L \mu_t \tau \right) \sum_{\mathbf{x} \in \mathcal{C}} \frac{|\mathcal{A}_{\tau,t}^{\mathbf{x}}|}{|\mathcal{A}_{\tau,t}|} \sum_{i=0}^{\tau-1} \frac{1}{|\mathcal{A}_{i,t}^{\mathbf{x}}|} \sum_{\mathbf{y} \in \mathcal{A}_{i,t}^{\mathbf{x}}} \mathbb{E} \left\{ \|\nabla F(\mathbf{w}_{\mathbf{y},i,t}^{\mathbf{x}})\|^2 \right\}. \quad (61)$$

Thus, under small enough μ_t and the following condition

$$1 - \frac{L^2 \mu_t^2 \tau (\tau - 1)}{2} - L \mu_t \tau \geq 0, \quad (62)$$

and the symmetry and independency of the network distribution for different intra- and inter-cluster iterations, which lead to (35)-(40) having the same value for all \mathbf{x} , \mathbf{y} , i and t , we obtain the following bound on (47)

$$\begin{aligned} \mathbb{E} \left\{ F(\mathbf{w}_{\mathbf{y}_0,0,t+1}^{\circ}) - F(\mathbf{w}_{\mathbf{y}_0,0,t}^{\circ}) \right\} &\leq -\frac{\mu_t \tau}{2} \mathbb{E} \left\{ \|\nabla F(\mathbf{w}_{\mathbf{y}_0,0,t}^{\circ})\|^2 \right\} \\ &+ \frac{L^2 \mu_t^3 \sigma^2 \tau (\tau - 1)}{2 B} \mathbb{E} \left\{ \frac{1}{|\mathcal{A}^{\circ}|} \right\} + \frac{L^2 \mu_t^3 \tau (\tau - 1)}{2} \mathbb{E} \left\{ \frac{1}{|\mathcal{A}^{\circ}|^2} \right\} \mathbb{E} \left\{ \|\epsilon_{\mathbf{u}}^{\circ}\|^2 \right\} \\ &+ \frac{L^2 \mu_t^3 \tau (\tau - 1)}{2} \mathbb{E} \left\{ \frac{1}{|\mathcal{A}^{\circ}|^2} \right\} \mathbb{E} \left\{ \|\epsilon_{\mathbf{d}_{\mathbf{y}_0}}^{\circ}\|^2 \right\} \\ &+ \frac{L^2 \mu_t \tau}{2} \mathbb{E} \left\{ \frac{1}{|\mathcal{A}|^2} \right\} \mathbb{E} \left\{ \|\epsilon_{\mathbf{d}_{\mathbf{y}_0}}\|^2 \right\} + \frac{L^2 \mu_t \tau}{2} \mathbb{E} \left\{ \frac{1}{|\mathcal{A}|^2} \right\} \mathbb{E} \left\{ \|\epsilon_{\mathbf{d}_{\mathbf{y}_0}}\|^2 \right\} \\ &+ \frac{L \mu_t^2 \sigma^2}{2 B} \tau \mathbb{E} \left\{ \frac{1}{|\mathcal{A}^{\circ}|} \right\} \mathbb{E} \left\{ \sum_{\mathbf{x} \in \mathcal{C}} \frac{|\mathcal{A}^{\mathbf{x}}|^2}{|\mathcal{A}|^2} \right\} + \frac{L \mu_t^2}{2} \tau \mathbb{E} \left\{ \frac{1}{|\mathcal{A}^{\circ}|^2} \right\} \mathbb{E} \left\{ \|\epsilon_{\mathbf{u}}^{\circ}\|^2 \right\} \mathbb{E} \left\{ \sum_{\mathbf{x} \in \mathcal{C}} \frac{|\mathcal{A}^{\mathbf{x}}|^2}{|\mathcal{A}|^2} \right\} \\ &+ \frac{L \mu_t^2}{2} \tau \mathbb{E} \left\{ \frac{1}{|\mathcal{A}|} \right\} \mathbb{E} \left\{ \frac{1}{|\mathcal{A}^{\circ}|^2} \right\} \mathbb{E} \left\{ \|\epsilon_{\mathbf{d}_{\mathbf{y}_0}}^{\circ}\|^2 \right\} + \frac{L}{2} \mathbb{E} \left\{ \frac{1}{|\mathcal{A}|} \right\} \mathbb{E} \left\{ \frac{1}{|\mathcal{A}|^2} \right\} \mathbb{E} \left\{ \|\epsilon_{\mathbf{d}_{\mathbf{y}_0}}\|^2 \right\} \\ &+ \frac{L}{2} \mathbb{E} \left\{ \frac{1}{|\mathcal{A}|^2} \right\} \mathbb{E} \left\{ \|\epsilon_{\mathbf{d}_{\mathbf{y}_0}}\|^2 \right\} + \frac{L}{2} \mathbb{E} \left\{ \frac{1}{|\mathcal{A}|^2} \right\} \mathbb{E} \left\{ \|\epsilon_{\mathbf{u}}\|^2 \right\} + \frac{L}{2} \mathbb{E} \left\{ \frac{1}{|\mathcal{A}|^2} \right\} \mathbb{E} \left\{ \|\epsilon_{\mathbf{d}_{\mathbf{y}_0}}\|^2 \right\}. \quad (63) \end{aligned}$$

Then, applying Assumption 3, we have for any $t \in \{0, \dots, T-1\}$

$$\begin{aligned} \mathbb{E} \left\{ F(\mathbf{w}_{\mathbf{y}_0,0,t+1}^{\circ}) \right\} - F^* &\leq (1 - \mu_t \tau \delta) \left(\mathbb{E} \left\{ F(\mathbf{w}_{\mathbf{y}_0,0,t}^{\circ}) \right\} - F^* \right) \\ &+ \frac{L^2 \mu_t^3 \sigma^2 \tau (\tau - 1)}{2 B} \mathbb{E} \left\{ \frac{1}{|\mathcal{A}^{\circ}|} \right\} + \frac{L \mu_t^2 \sigma^2}{2 B} \tau \mathbb{E} \left\{ \frac{1}{|\mathcal{A}^{\circ}|} \right\} \mathbb{E} \left\{ \sum_{\mathbf{x} \in \mathcal{C}} \frac{|\mathcal{A}^{\mathbf{x}}|^2}{|\mathcal{A}|^2} \right\} \\ &+ \mathbb{E} \left\{ \frac{1}{|\mathcal{A}^{\circ}|^2} \right\} \left(\frac{L^2 \mu_t^3 \tau (\tau - 1)}{2} + \frac{L \mu_t^2}{2} \tau \mathbb{E} \left\{ \sum_{\mathbf{x} \in \mathcal{C}} \frac{|\mathcal{A}^{\mathbf{x}}|^2}{|\mathcal{A}|^2} \right\} \right) \mathbb{E} \left\{ \|\epsilon_{\mathbf{u}}^{\circ}\|^2 \right\} \\ &+ \mathbb{E} \left\{ \frac{1}{|\mathcal{A}^{\circ}|^2} \right\} \left(\frac{L^2 \mu_t^3 \tau (\tau - 1)}{2} + \frac{L \mu_t^2}{2} \tau \mathbb{E} \left\{ \frac{1}{|\mathcal{A}|} \right\} \right) \mathbb{E} \left\{ \|\epsilon_{\mathbf{d}_{\mathbf{y}_0}}^{\circ}\|^2 \right\} \\ &+ \mathbb{E} \left\{ \frac{1}{|\mathcal{A}|^2} \right\} \left(L^2 \mu_t \tau + \frac{L}{2} \mathbb{E} \left\{ \frac{1}{|\mathcal{A}|} \right\} + L \right) \mathbb{E} \left\{ \|\epsilon_{\mathbf{d}_{\mathbf{y}_0}}\|^2 \right\} \\ &+ \frac{L}{2} \mathbb{E} \left\{ \frac{1}{|\mathcal{A}|^2} \right\} \mathbb{E} \left\{ \|\epsilon_{\mathbf{u}}\|^2 \right\}. \quad (64) \end{aligned}$$

This bound connects the inter-cluster iterative steps $t + 1$ and t . To get the bound of Theorem 1, we can replace $\mathbb{E} \{F(\mathbf{w}_{\mathbf{y}_0,0,t}^o)\} - F^*$ on RHS with the same one step bound for t and $t - 1$. Repeating the procedure over $\{t - 1, \dots, 0\}$, and from the equality $\sum_{i=0}^{t-1} c^i = \frac{1-c^t}{1-c}$ for any $c < 1$, the proof is complete.

REFERENCES

- [1] J. Park, S. Samarakoon, M. Bennis, and M. Debbah, "Wireless network intelligence at the edge," *Proceedings of IEEE*, vol. 107, no. 11, pp. 2204-2239, Nov. 2019.
- [2] H. Hellstrom, J. M. B. da Silva Jr, M. M. Amiri, M. Chen, V. Fodor, H. V. Poor, and C. Fischione, "Wireless for machine learning: A survey," *Foundations and Trends® in Signal Processing*, vol. 15, no. 4, pp. 290-399, 2022.
- [3] B. McMahan, E. Moore, D. Ramage, S. Hampson, and B. A. Arcas, "Communication-efficient learning of deep networks from decentralized data," *AISTATS*, pp. 1273-1282, 2017.
- [4] M. Chen, D. Gunduz, K. Huang, W. Saad, M. Bennis, A. V. Feljan, and H. V. Poor, "Distributed learning in wireless networks: Recent progress and future challenges," *IEEE J. Sel. Areas Commun.*, vol. 39, no. 12, pp. 3579-3605, Dec. 2021.
- [5] M. Mohammadi Amiri and D. Gunduz, "Machine learning at the wireless edge: Distributed stochastic gradient descent over-the-air," *IEEE Trans. Signal Proc.*, vol. 68, pp. 2155-2169, Mar. 2020.
- [6] M. Mohammadi Amiri and D. Gunduz, "Federated learning over wireless fading channels," *IEEE Trans. Wireless Commun.*, vol. 19, no. 5, pp. 3546-3557, May 2020.
- [7] M. Chen, Z. Yang, W. Saad, C. Yin, H. V. Poor, and S. Cui, "A joint learning and communications framework for federated learning over wireless networks," *IEEE Trans. Wireless Commun.*, vol. 20, no. 1, pp. 269-283, Dec. 2021.
- [8] L. Liu, J. Zhang, S. H. Song, and K. B. Letaief, "Hierarchical federated learning with quantization: Convergence analysis and system design," *IEEE Trans. Wireless Commun.*. Early Access: <https://ieeexplore.ieee.org/document/9834296>
- [9] S. Liu, G. Yu, X. Chen, and M. Bennis, "Joint user association and resource allocation for wireless hierarchical federated learning with IID and non-IID data" *IEEE Trans. Wireless Commun.*. Early Access: <https://ieeexplore.ieee.org/document/9748976>
- [10] S. Luo, X. Chen, Q. Wu, Z. Zhou, and S. Yu, "HFEL: Joint edge association and resource allocation for cost-efficient hierarchical federated edge learning," *IEEE Trans. Wireless Commun.*, vol. 19, no. 10, pp. 6535-6548, Oct. 2020.
- [11] L. Liu, J. Zhang, S. H. Song, and K. B. Letaief, "Client-edge-cloud hierarchical federated learning," *IEEE Int. Conf. Commun. (ICC)*, Jun. 2020.
- [12] O. Aygun, M. Kazemi, D. Gunduz, and T. M. Duman, "Hierarchical over-the-air federated edge learning," *IEEE Int. Conf. Commun. (ICC)*, May 2022.
- [13] S. Zheng, C. Shen, and X. Chen, "Design and analysis of uplink and downlink communications for federated learning," *IEEE J. Sel. Areas Commun.*, vol. 39, no. 7, pp. 2150-2167, July 2021.
- [14] Q. Zeng, Y. Du, K. Leung, and K. Huang, "Energy-efficient resource management for federated edge learning with CPU-GPU heterogeneous computing," *IEEE Trans. Wireless Commun.*, vol. 20, no. 12, pp. 7947-7962, Dec. 2021.
- [15] B. Nazer and M. Gastpar, "Computation over multiple-access channels," *IEEE Trans. Inf. Theory*, vol. 53, no. 10, pp. 3498-3516, Oct. 2007.
- [16] S. M. Azimi-Abarghouyi, M. Hejazi, B. Makki, M. Nasiri-Kenari, and T. Svensson, "Decentralized compute-and-forward for ad hoc networks," *IEEE Wireless Commun. Lett.*, vol. 5, no. 6, pp. 652-655, Dec. 2016.

- [17] K. Yang, T. Jiang, Y. Shi, and Z. Ding, "Federated learning via over-the-air computation," *IEEE Trans. Wireless Commun.*, vol. 19, no. 3, pp. 2022-2035, Mar. 2020.
- [18] G. Zhu, Y. Wang, and K. Huang, "Broadband analog aggregation for low-latency federated edge learning," *IEEE Trans. Wireless Commun.*, vol. 19, no. 1, pp. 491-506, Jan. 2020.
- [19] Z. Lin, X. Li, V. K. N. Lau, Y. Gong, and K. Huang, "Deploying federated learning in large-scale cellular networks: Spatial convergence analysis," *IEEE Trans. Wireless Commun.*, vol. 21, no. 3, pp. 1542-1556, Mar. 2022.
- [20] G. Zhu, Y. Du, D. Gunduz, and K. Huang, "One-bit over-the-air aggregation for communication-efficient federated edge learning: Design and convergence analysis," *IEEE Trans. Wireless Commun.*, vol. 20, no. 3, pp. 2120-2135, Mar. 2021.
- [21] X. Cao, G. Zhu, J. Xu, Z. Wang, and S. Cui, "Optimized power control design for over-the-air federated edge learning," *IEEE J. Sel. Areas Commun.*, vol. 40, no. 1, pp. 342-358, Jan. 2022.
- [22] G. Zhu, J. Xu, K. Huang, and S. Cui, "Over-the-air computing for wireless data aggregation in massive IoT," *IEEE Wireless Commun. Mag.*, vol. 28, no. 4, pp. 57-65, Aug. 2021.
- [23] M. Mohammadi Amiri, D. Gunduz, S. R. Kulkarni, and H. V. Poor, "Convergence of federated learning over a noisy downlink," *IEEE Trans. Wireless Commun.*, vol. 21, no. 3, pp. 1422-1437, Mar. 2022.
- [24] Z. Wang, Y. Zhou, Y. Shi, and W. Zhuang, "Interference management for over-the-air federated learning in multi-cell wireless networks," *IEEE J. Sel. Areas Commun.*, vol. 40, no. 8, pp. 2361-2377, Aug. 2022.
- [25] M. Haenggi, *Stochastic Geometry for Wireless Networks*. Cambridge University Press, 2012.
- [26] S. M. Azimi-Abarghouyi, B. Makki, M. Haenggi, M. Nasiri-Kenari, and T. Svensson, "Stochastic geometry modeling and analysis of single- and multi-cluster wireless networks," *IEEE Trans. Commun.*, vol. 66, no. 10, pp. 4981-4996, Oct. 2018.
- [27] S. M. Azimi-Abarghouyi and H. S. Dhillon, "Matérn cluster process with holes at the cluster centers," available on arXiv: <https://arxiv.org/abs/2210.06065>
- [28] S. M. Azimi-Abarghouyi, M. Nasiri-Kenari, and M. Debbah, "Stochastic design and analysis of user-centric wireless cloud caching networks," *IEEE Trans. Wireless Commun.*, vol. 19, no. 7, pp. 4978-4993, July 2020.
- [29] S. M. Azimi-Abarghouyi, H. S. Dhillon, and L. Tassiulas, "Fundamentals of clustered molecular nanonetworks," available on arXiv: <https://arxiv.org/pdf/2208.14213>
- [30] C. Hou, K. K. Thekumparampil, G. Fanti, and S. Oh, "FeDChain: Chained algorithms for near-optimal communication cost in federated learning," *ICLR*, Lisbon, Portugal, Oct. 2022.
- [31] J. G. Andrews, F. Baccelli, and R. K. Ganti, "A tractable approach to coverage and rate in cellular networks," *IEEE Trans. Commun.*, vol. 59, no. 11, pp. 3122-3134, Nov. 2011.
- [32] H. Karimi, J. Nutini, and M. Schmidt, "Linear convergence of gradient and proximal-gradient methods under the Polyak-Lojasiewicz condition," in *Machine Learning and Knowledge Discovery in Databases* (Lecture Notes in Computer Science), pp. 795-811, 2016.
- [33] N. H. Tran, W. Bao, A. Zomaya, M. N. H. Nguyen, and C. S. Hong, "Federated learning over wireless networks: Optimization model design and analysis," *IEEE Int. Conf. Computer Commun. (INFOCOM)*, pp. 1387-1395, Apr. 2019.
- [34] Y. Lecun, "The MNIST database of handwritten digits," <http://yann.lecun.com/exdb/mnist/>, 1998.